CHARACTERIZING GREENHOUSE GAS EMISSIONS FROM FEED YARD OPERATIONS: METHODS AND GOVERNING FACTORS

A Thesis

by

KEITH MICHAEL HAMILTON

Submitted to the Office of Graduate and Professional Studies of
Texas A&M University
in partial fulfillment of the requirements for the degree of

MASTER OF SCIENCE

Chair of Committee,	Ronald E. Lacey
Committee Members,	Sarah D. Brooks
	Gerald L. Riskowski
Head of Department,	Stephen W. Searcy

December 2017

Major Subject: Biological and Agricultural Engineering

ABSTRACT

In this research, the uncertainty of commonly used GHG measurement methods was evaluated using Taylor series uncertainty analysis and a field study was performed to evaluate the feasibility of one of these methods.

Taylor series uncertainty analysis was performed on three source-integrated methods: monostatic and bistatic open-path Fourier Transform Infrared Spectroscopy (OP-FTIR) and open-path tunable diode laser absorption spectroscopy (OP-TDLAS), and two source-specific methods: non-flow-through non-steady-state (NFT-NSS) and flow-through steady-state (FT-SS) chambers. The average systematic uncertainty for the three source-integrated methods was the same, 15.2%, when determining emission factors for methane (CH_4) and nitrous oxide (N_2O), except for OP-TDLAS, which did not measure N_2O. When determining emission factors from source-specific measurements, NFT-NSS chambers had an average systematic uncertainty of 21.2% and 24.6% for CH_4 and N_2O, respectively. The FT-SS chambers had an average systematic uncertainty of 13.5% when determining emission factors for CH_4 and N_2O by a single flux chamber measurement.

A field study was conducted in the high plains of Texas at a feed yard with a potential maximum capacity of 50,000 head of cattle. The objective of this study was to determine the feasibility of using an OP-FTIR system to characterize emissions from a ground-level area source with precision. The feed yard was partitioned into multiple sources of CH_4 and N_2O that included enteric fermentation from the cattle, the manure in the pens, silage storage, manure storage, and a storage lagoon for runoff water from the pens. A bistatic OP-FTIR was placed 27 meters (m) north and parallel to the cattle pens

with a path length of 550 m. A meteorological station was also located on this side of the feed yard, 5 meters north of the OP-FTIR path length.

The 1-hour average CH_4 concentrations were 1.62-6.87 ppm and 1.36-4.97 ppm for downwind and upwind measurements, respectively. Measured 1-hour average N_2O concentrations were 168-514 ppb and 203-530 ppb for downwind and upwind measurements, respectively. The downwind and upwind N_2O measurements could not be statistically differentiated with the use of a single OP-FTIR system.

CONTRIBUTORS AND FUNDING SOURCES

Contributors

This work was supported by a thesis committee consisting of Dr. Ronald Casey and Dr. Gerald Riskowski of the Department of Biological and Agricultural Engineering, and Professor Sarah Brooks of the Department of Atmospheric Sciences.

The data analyzed for Chapter 2 was provided by Dr. Ken Casey and Dr. Saidul Borhan. All other work conducted for the thesis was completed by the student independently.

Funding Sources

Graduate study was supported by a fellowship from Texas A&M University.

NOMENCLATURE

BACT	Best Available Control Technology
CH_4	Methane
CAA	Clean Air Act
CO_2	Carbon dioxide
CO_2e	Carbon dioxide equivalents
ECD	Electron capture detector
EPA	United States Environmental Protection Agency
FID	Flame ionization detector
FT-SS	Flow-through steady-state
GC	Gas chromatograph
GHG	Greenhouse gas
GWP	Global warming potential
IPCC	Intergovernmental Panel on Climate Control
IR	Infrared
LMC	Line of maximum concentration
MRR	EPA's Mandatory Reporting of Greenhouse Gases Final Rule
N_2O	Nitrous Oxide
NFT-NSS	Non-flow-through non-steady state
OP-FTIR	Open-path Fourier Transform Infrared Spectroscopy
OP-TDLAS	Open-path tunable diode laser absorption spectroscopy

PSD	Prevention of Significant Deterioration
US	United States

TABLE OF CONTENTS

Page

LIST OF FIGURES

Page

LIST OF TABLES

Page

CHAPTER I

INTRODUCTION

Increased focus on greenhouse gas (GHG) emissions has led to required reporting of emissions from industrial and agricultural sources. In 2009, the United States (US) Environmental Protection Agency (EPA) issued the Mandatory Reporting of Greenhouse Gases Rule (FR 74 at 56373) which requires reporting of all GHG emission from sources emitting more than 25,000 metric tons of carbon dioxide equivalents (CO_2e) per year, where a CO_2e is defined as a compound's global warming potential (GWP) compared to carbon dioxide (CO_2). The purpose of the rule is "to collect accurate and timely GHG information for future regulation and policy decisions" (FR 74 at 56373). Subpart JJ of the rule requires agricultural industries emitting 25,000 metric tons or more of CO_2e per year from manure management practices to report these emissions based on emission factors developed by the Intergovernmental Panel on Climate Change (IPCC). Emissions resulting from enteric fermentation are not subject to reporting requirements because practical methods to estimate enteric fermentation emissions are difficult to implement and fraught with uncertainty (FR 74 at 56373). The compounds of interest in agriculture are carbon dioxide (CO_2), methane (CH_4), and nitrous oxide (N_2O). Methane (CH_4) and N_2O have CO_2e of 21 and 310, respectively (FR 74 at 56373).

Under the current rule, agricultural emissions are estimated using IPCC emission factors with uncertainties of ±30% to ±50% (Eggleston et al., 2006). These emission factors were established in the 1990's with methods and equipment that were less precise than modern instrumentation and based on agricultural operations that are managed

differently than those in the US; therefore, such emission factors may not represent modern US production and management practices. If emission factors applicable to US agriculture are not correctly identified, improper regulation of emitting operations may result once GHG regulations are implemented.

Quantifying GHG emissions from agricultural ground-level area sources such as feed yard operations is challenging because of the temporal and spatial heterogeneity of emissions. At a feed yard operation, many diverse sources of GHGs are located in an expansive open environment, making it costly and difficult to accurately characterize emissions from any one specific source. The generation of GHGs from manure management is dependent on many factors including surface temperature, pH, carbon-to-nitrogen and water-to-solids ratios, nutrient composition, particle size, retention time and more which makes it difficult to develop a reliable emission factor for an ever-changing environment (Weiske et al., 2005).

Literature Review

The use of nitrogen fertilizer in North America has stabilized, causing the contribution of GHG emissions from crops to be stagnant. This leaves the main increase of agricultural GHG emissions to management practices of cattle, poultry, and swine manure. The IPCC stated that increased global beef demand will cause increased emissions of CH_4 and N_2O. Rumination from cattle and sheep is a large source of CH_4 that can be mitigated through feeding practices, dietary additives, long term management changes, and animal breeding. Animal manures can release significant amounts of CH_4

and N_2O during storage, but the magnitude of these emissions varies with environmental conditions (IPCC, 2007).

In the 2009 Endangerment Finding (FR 74 at 66496), Administrator Jackson concluded GHGs are a danger to public health and welfare and are required to be regulated under the Clean Air Act (CAA). The Prevention of Significant Deterioration (PSD) program states if any of the criteria pollutants classified in the CAA are emitted in the amount of 100 tons per year (tpy) or 250 tpy, depending on the type of source, that source must obtain an operating permit (FR 74 at 66496). If these thresholds were applied to GHGs, millions of small sources would be subject to regulation under the PSD program resulting in a gridlock of the PSD program and would not have the desired effect on GHG emissions (FR 74 at 66496). To manage the increased burden associated with regulation of GHGs, EPA finalized a GHG Tailoring Rule in May 2010 to be implemented in two phases that adjusts these thresholds for GHGs to 100,000 tpy CO_2e for new sources and 75,000 tpy CO_2e for existing facilities that have undergone modifications (FR 74 at 66496). In the first phase, sources currently subject to PSD permitting will, in addition, be subject to permit requirements for GHGs. These additional requirements are for any facility with an increase of 75,000 tpy CO_2e to utilize Best Available Control Technology (BACT) to lower emissions. This phase became effective January 2, 2011. The second phase will require newly constructed facilities emitting more than 100,000 tpy CO_2e to be subject to PSD permitting requirements even if solely on GHG emissions.

Rationale and Significance

The magnitude of emissions from all GHG sources needs to be accurately assessed in order to be prepared for upcoming legislation on GHG abatement. The work in this document is to determine a reliable and accurate method for measuring GHG emissions from spatially and temporally heterogeneous sources, such as feed yards. As an example of a method for achieving these ends, emissions from a feed yard were characterized using continuous concentrations supplied by a single open-path Fourier transform infrared spectrometers (OP-FTIR).

Objectives

The goal of this research was to evaluate methods for GHG emission measurement from ground-level area sources. Specifically, the objectives of this research were:

1. Determine a preferred method for GHG emission measurement from large area sources among the methods described in Table 1 by the following steps:
    - Perform Taylor series uncertainty analysis of methods with GHG concentrations datasets obtained through experimental measurement and literature review.
    - Categorize and rank methods based on total overall uncertainty, primary variable contributions, and advantages/disadvantages.
2. Determine factors that contribute to fluctuations of CH_4 and N_2O concentrations from large area sources, specifically feed yards, by the following steps:

- Deploy a bistatic OP-FTIR spectrometer and meteorological station at a feed yard in the high plains of Texas to collect GHG concentrations and meteorological data.
- Utilize multivariable statistical methods to determine contributing meteorological variables to fluctuations of CH_4 and N_2O concentrations.

Methods

Objective 1

A variety of measurement methods have been used at various industrial facilities for the reporting of total emissions. Through review of the literature, the most common methods for measuring GHG emissions from ground-level area sources were identified with a focus on CH_4 and N_2O (Table 1) to characterize the systematic uncertainties associated with emission rates and assay the advantages and disadvantages of each method. The methods can be categorized into two groups: source-integrated and source-specific methods. Source-integrated methods measure a concentration downwind of the site under investigation and require reverse calculation using an air dispersion model to determine the emission rate of the source. The resulting measurement includes emissions from all contributing sources on the site. This method cannot address problems where only one source among many is in question.

Source-specific methods measure emission rates directly at each source and do not require air dispersion modeling. Measurements are taken of emissions from a smaller area

of a larger source, resulting in an emission rate that may not accurately describe a complex, spatially and temporally heterogeneous area source. The source-specific flux chamber methods also create microenvironments during measurement that may alter emissions from the source.

Table 1. References for common methods for GHG measurement.

	Method	Reference(s)
Source-Integrated	Bistatic OP-FTIR	Hashmonay et al., 1999
	Monostatic OP-FTIR	Bjorneberg et al., 2009; Kirchgessner et al., 1993; Reese et al., 2009; Shores et al., 2005
	OP-TDLAS	Kyoung et al., 2007; Modrak et al., 2005
Source-specific	FT-SS chamber	Borhan et al., 2011
	NFT-NSS chamber	Parkin and Venterea, 2010

Source-integrated methods evaluated were monostatic and bistatic OP-FTIR, and open-path tunable diode laser absorption spectroscopy (OP-TDLAS). Source-specific methods evaluated included non-flow-through non-steady-state (NFT-NSS) and flow-through steady-state (FT-SS) chambers coupled with gas chromatography. A Taylor series uncertainty analysis (Taylor and Kuyatt, 1994) was applied to each method to estimate the overall systematic uncertainty of calculated CH_4 and N_2O emission rates, assuming representative uncertainties in primary measurements and each method's relative sensitivity to its respective primary measurements. Methods were characterized

based on their maximum potential uncertainty and advantages and disadvantages when measuring GHG emissions from large, spatially and temporally heterogeneous area sources common in US animal production.

Objective 2

Ideally, two OP-FTIR systems would be deployed at a feed yard in the high plains of Texas, one upwind and the other downwind of the yard to record differential concentrations from the feed yard at the same time. Because of financial limitations in this study, a single system was deployed at the north side of the feed yard. The upwind measurement was assumed to be the background concentrations (i.e. ambient for the surrounding area) and constant throughout the measurement period. Any increases in concentrations in the downwind measurement were assumed to originate from the feed yard. The OP-FTIR system (Model: M4413-F, MIDAC Corp., Westfield, MA) was a bistatic system with a separate infrared source from the interferometer. This type of system allows for a longer path length over its monostatic counterpart. Monostatic systems have the infrared source and interferometer as one unit; retro-reflectors are used to reflect the infrared signal back to the interferometer in order to determine total absorbance of infrared energy by the gaseous compounds within the path length. The system monitored CH_4 and N_2O concentrations on a continuous basis over a two-year period.

As a result of the high dust environment near the feed yard, the OP-FTIR system was fitted with protective shielding to minimize maintenance and was secured to a trailer

for mobility. The trailer was supported on metal stands constructed to bolt to 3-foot-deep concrete piers to maintain a stable base for the interferometer. The infrared source was also secured to a trailer and anchored in the same fashion. The OP-FTIR system had a single computer station on the spectrometer trailer to log data and operate the system using a program called AutoQuant Pro (ver. 4.0, MIDAC Corp., Westfield, MA). This software was used to operate the OP-FTIR and analyze the spectra produced by the system. The computer station was enclosed in a climate-controlled box to protect it from the surrounding environment.

A weather station measuring temperature, relative humidity, barometric pressure, precipitation, solar radiation, and wind speed and direction was deployed on the downwind side of the feed yard. The meteorological data and concentrations were collected on minute intervals. The meteorological data collected were paired with the measured concentrations and analyzed with multivariable statistical techniques to determine the contributing factors to CH_4 and N_2O concentrations. This information will provide a better understanding of GHG emissions from large agricultural area sources.

CHAPTER II

EVALUATION OF METHODS FOR CHARACTERIZING GREENHOUSE GAS EMISSIONS FROM FEED YARDS

Introduction

Increased focus on greenhouse gas (GHG) emissions has led to required reporting of emissions from industrial and agricultural sources. In 2009, the United States (US) Environmental Protection Agency (EPA) issued the Mandatory Reporting of Greenhouse Gases Rule (FR 74 at 56373) which requires reporting of all GHG emission from sources emitting more than 25,000 metric tons of carbon dioxide equivalents (CO_2e) per year, where a CO_2e is defined as a compound's global warming potential (GWP) compared to carbon dioxide (CO_2). The purpose of the rule is "to collect accurate and timely GHG information for future regulation and policy decisions" (FR 74 at 56373). Subpart JJ of the rule requires agricultural industries emitting 25,000 metric tons or more of CO_2e per year from manure management practices to report these emissions based on emission factors developed by the Intergovernmental Panel on Climate Change (IPCC). Emissions resulting from enteric fermentation are not subject to reporting requirements because practical methods to estimate enteric fermentation emissions are difficult to implement and fraught with uncertainty (FR 74 at 56373). The compounds of interest in agriculture are carbon dioxide (CO_2), methane (CH_4), and nitrous oxide (N_2O). Methane (CH_4) and N_2O have CO_2e of 21 and 310, respectively (FR 74 at 56373).

Under the current rule, agricultural emissions are estimated using IPCC emission factors with uncertainties of ±30% to ±50% (Eggleston et al., 2006). These emission factors were established in the 1990's with methods and equipment that were less precise than modern instrumentation and based on agricultural operations that are managed differently than those in the US; therefore, such emission factors may not represent modern US production and management practices. If emission factors applicable to US agriculture are not correctly identified, improper regulation of emitting operations may result once GHG regulations are implemented.

Quantifying GHG emissions from agricultural ground-level area sources such as feed yard operations is challenging because of the temporal and spatial heterogeneity of emissions. At a feed yard operation, many diverse sources of GHGs are located in an expansive open environment, making it costly and difficult to accurately characterize emissions from any one specific source. The generation of GHGs from manure management is dependent on many factors including surface temperature, pH, carbon-to-nitrogen and water-to-solids ratios, nutrient composition, particle size, retention time and more which makes it difficult to develop a reliable emission factor for an ever-changing environment (Weiske et al., 2005).

A variety of measurement methods have been used to determine GHG emissions from various industrial facilities for the reporting of the total emissions. Through review of the literature, common methods for measuring GHG emissions from ground-level area sources have been identified with an emphasis on CH_4 and N_2O. The objective of this study was to characterize the systematic uncertainties associated with emission factors

determined using common measurement techniques while exploring the advantages and disadvantages of each method.

Measurement Methods Analyzed

The methods investigated in this study were categorized into two groups: source-integrated and source-specific methods.

Source-integrated methods utilize concentrations measured downwind of the sources under investigation and require reverse air dispersion modeling to determine the emission factors for constituents from the sources of interest. Source-integrated methods evaluated in this study include monostatic and bistatic open-path Fourier Transform Infrared Spectroscopy (OP-FTIR) and open-path tunable diode laser absorption spectroscopy (OP-TDLAS). The resulting measurement of a source-integrated method encompasses emissions from all sources present at a given facility, creating an issue when only one source is in question (e.g., when trying to differentiate CH_4 emissions from manure management versus enteric fermentation).

Source-specific methods measure emission factors directly at the source and do not require modeling. Source-specific methods evaluated include non-flow-through non-steady-state (NFT-NSS) and flow-through steady-state (FT-SS) chambers analyzed using gas chromatography. Source-specific methods measure emissions from a small area of a larger source, resulting in an emission factor that may not accurately describe a complex, spatially and temporally heterogeneous area source. In addition, the source-specific

chamber methods under evaluation create microenvironments during measurement that may alter emissions from the emitting source (Rochette, 2011).

Data regarding use of each method were collected from the sources identified in Table 1. A Taylor series uncertainty analysis (Taylor and Kuyatt, 1994) was applied to each method to determine the overall systematic uncertainty of calculated emission factors of CH_4 and N_2O. The OP-TDLAS were only evaluated for CH_4 because there are currently no open-path TDLAS systems capable of accurately measuring N_2O concentrations. Methods were characterized based on their maximum potential uncertainty as well as advantages and disadvantages when measuring GHG emissions from large, spatially and temporally heterogeneous area sources common in US animal production.

Methods

Taylor Series Uncertainty Analysis

A Taylor series uncertainty analysis (Taylor and Kuyatt, 1994) is a widely-used method for characterizing systematic uncertainty recommended by the National Institute of Standards and Technology. The Taylor series uncertainty analysis was used to estimate the total systematic uncertainty of CH_4 and N_2O emission factors calculated from each measurement method, and to estimate the representative measures of uncertainty in each primary measurement. The Taylor series uncertainty analysis states that when a measured

variable, Y, cannot be measured directly, it is determined by a number of independent variables, x_1, x_2, x_3, … , x_N, through a functional relation, *f* (Equation 1):

$$Y = f(x_1, x_2, x_3, \ldots, x_N) \tag{1}$$

Each independent variable, x_i, has an associated uncertainty, ω_i, where i ranges between 1 and N variables. The variable ω_Y represents the systematic uncertainty of Y resulting from the propagation of uncertainties in each independent variable and is calculated as the positive square root of the estimated variance, ω_Y^2 (Equation 2) (Holman, 2011):

$$\omega_Y = +\sqrt{\omega_Y^2} \tag{2}$$

where the variance, ω_Y^2, is calculated with Equation 3:

$$\omega_Y^2 = (\theta_1\omega_1)^2 + (\theta_2\omega_2)^2 + \ldots + (\theta_N\omega_N)^2 \tag{3}$$

The sensitivity coefficient, θ_i, is the ratio of the change of the result per unit change of a single input parameter (Equation 4):

$$\theta_i = \frac{\partial Y}{\partial x_i} \tag{4}$$

The contribution of uncertainty from each primary measurement to the overall uncertainty of the result is calculated by dividing the absolute systematic contribution of a single measurement, U_i, by the total absolute systematic uncertainty (Equation 5):

$$\%\ \text{Contribution} = \frac{U_i}{\sum_{i=1}^{N} U_i} \cdot 100\% \tag{5}$$

where the absolute systematic uncertainty contribution, U_i, of a primary measurement is determined according to Equation 6:

$$U_i = \left(\frac{\omega_i}{2} \cdot \theta_i\right)^2 \quad (6)$$

Measurement Methods

OP-FTIR

An OP-FTIR system utilizes an infrared (IR) beam directed toward a spectrometer to measure concentrations of multiple gases simultaneously. Between the source of the IR beam and spectrometer, compounds in the air absorb a portion of the IR signal at specific wavenumbers respective to the compounds present. The spectrometer quantifies the absorbance of IR energy based on the presence of the compounds into an absorbance spectrum. This absorbance spectrum can be compared to reference spectra to determine concentrations of specific compounds in the IR beam's path. The advantage of an OP-FTIR system is the capability of measuring multiple compounds simultaneously through an accurate, non-invasive process (MIDAC, 2008).

A monostatic OP-FTIR system consists of a spectrometer and IR source combined into a single unit. This unit is aligned with a retroreflector to reflect the IR signal created by the IR source back to the spectrometer. The two instruments are aligned such that the plume from the area source passes through the IR path. A monostatic system is advantageous when a limited power source is available or if radial plume mapping is used. Radial plume mapping uses multiple path vectors to encompass a cross sectional area of a

plume in three dimensions to better characterize the dispersion of the concentration in the plume (Hashmonay, 2008). With a bistatic system, multiple IR sources would be required for an analytical procedure such as radial plume mapping, quickly increasing the cost of instrumentation and the required number of power sources. In a monostatic OP-FTIR system the IR beam is reflected over the path length a second time before reaching the detector for analysis (Figure 1, bottom) (Russwurm and Childers, 1996). This property of the monostatic system decreases the measured path length by at least half. A limited path length can be an issue when evaluating an area source with a wide plume, such as a feed yard. A decrease in accuracy of approximately 50% is realized when compared to a bistatic system because of the requirement to use a retroreflector with a monostatic system (Steve Plowman, MIDAC Corp., personal communication, May 2, 2011).

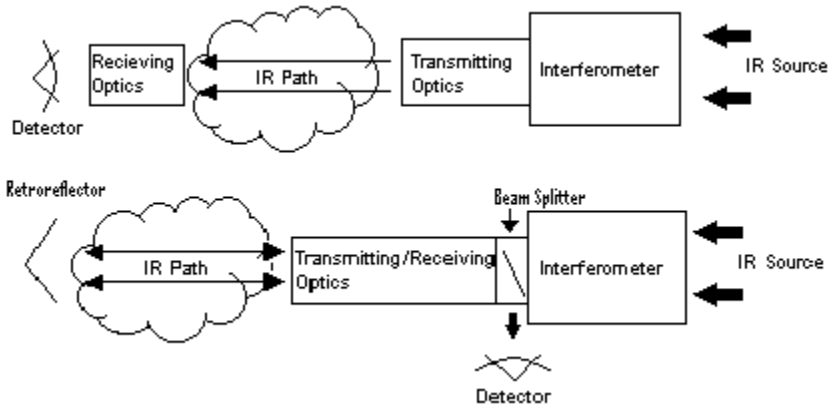

Figure 1. Bistatic (top) and monostatic (bottom) OP-FTIR systems.

The bistatic OP-FTIR system operates much like the monostatic system except the spectrometer and source are two separate units aligned with one another directly rather

than using a retroreflector (Figure 1, top). These changes allow the system to implement a longer path length than its monostatic counterpart. An OP-FTIR system produces an absorbance spectrum that can be analyzed to determine the average concentrations of measured compounds within the path length, so in order to obtain representative measurements it is important to encompass as much of the plume as possible within the path length (ASTM, 2007).

Independent of type, OP-FTIR systems do not require frequent calibration with reference gases. OP-FTIR systems use well maintained databases of reference spectra to compare with collected data to quantify concentrations of compound of interest.

OP-TDLAS

An OP-TDLAS is an instrument much like the OP-FTIR systems in which retroreflectors are positioned such that the gas plume under investigation passes through the path between the TDLAS and retroreflectors. This system measures the average concentration of a specific compound within the path length. An OP-TDLAS system is less expensive than a comparable OP-FTIR, however, it is normally calibrated to measure only one to three compounds at a time. The potential error of an OP-TDLAS is increased with the addition of each calibrated compound (Thoma et al., 2005). OP-FTIR and OP-TDLAS systems can procure highly time-resolved measurements, and measurements are inexpensive after initial capital costs are incurred.

Reverse Air Dispersion Model

Reverse air dispersion modeling is the process of calculating an emission rate for source based on a concentration measured by downwind monitoring equipment (Flesch et. al., 2007). Source-integrated methods require reverse air dispersion modeling to determine an emission rate from a measured concentration. Meteorological conditions at the time of measurement are used in the reverse air dispersion model to evaluate dispersion of the gaseous compound. In this study, a Gaussian air dispersion model was evaluated while representing the area source as a series of line sources, much like is done by ISCST3 or EPA's preferred regulatory model, AERMOD.

In order to evaluate an area source, two integrals are evaluated by the Gaussian model to account for the dimension of the source. The first integral evaluates the dimension perpendicular with the wind direction and the second integral evaluates the dimension parallel with the wind direction. This technique was not used in this study because it is not possible to evaluate this second integral without using a trapezoidal estimation of the integral (EPA, 1995) and the Taylor series uncertainty analysis is not able to a characterize a trapezoidal estimation directly. Therefore, the area source was represented as a series of line sources.

The two methods of representing the area source (i.e., using double integrals and using a series of line sources) were evaluated using AERMOD (v.12060) and it was determined the results are reasonably similar (within 5% of each other). This comparison was performed by representing the dimensions of the feed yard by 10 evenly spaced line sources with a uniform emission rate. A single receptor was centered in the east-west

direction and 28 meters north of the feed yard. The modeled concentration at the receptor was compared to a model analysis with the feed yard represented as an area source. The receptor placement, emission rate, and meteorological data were identical in both analyses.

It was determined during the Taylor series uncertainty analysis that the systematic uncertainty would approach infinity when evaluating the full extent of the area source. This would occur when evaluating regions of the source that did not contribute measurably to the observed concentration because the plume from that portion of the source did not intersect the measurement path. Therefore, only areas of the source known to contribute to the measurable concentration were evaluated. As shown in Figure 2, the section of the area source within 200 meters of the receptor contributes to approximately 80% of measured emissions from the area source (Faulkner et al., 2007).

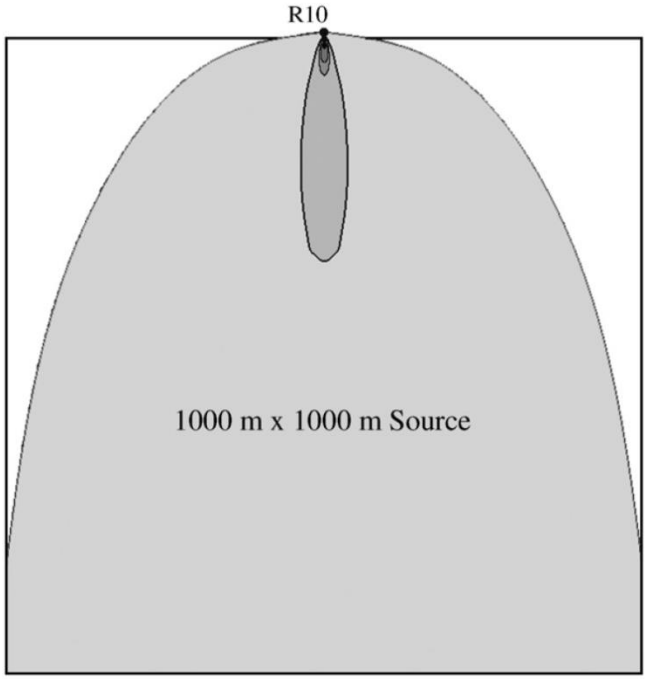

Figure 2. Contributing portions of a 1000 x 1000 m source to a sampler placed 10 m from the source boundary described by isopleths of equal contributions (Faulkner et al., 2007). Greater contribution per unit area is demonstrated by the darker areas.

The emission rate from the area source was determined with Equation 7 (Cooper and Alley, 2002).

$$ER = C_{mass} \cdot U \cdot \sigma_y \cdot \sigma_z \cdot \pi \left[\int_{y1}^{y2} e^{\left(\frac{y^2}{2 \cdot \sigma_y^2} \right)} dy \right]^{-1} \quad (7)$$

Where ER is the emission rate of the area source (microgram per second, µg/s), C_{mass} is the measured concentration of compound downwind from the area source (microgram per cubic meter, $\mu g/m^3$), U is wind velocity (meter per second, m/s), y is the distance from the ends of the line source to the point of the measured concentration

perpendicular to the wind direction (meter, m), σ_y is the horizontal dispersion coefficient (m), and σ_z is the vertical dispersion coefficient (m).

The source-integrated instruments measure concentration in parts per million (ppm), therefore Equation 8 was used to convert the measured concentration into the units required by the reverse air dispersion modeling process.

$$C_{mass} = C_{ppm} \cdot MW \cdot \frac{P}{R \times T} \cdot 1000 \quad (8)$$

Where C_{ppm} is the measured concentration from the area source as it is displayed by the measurement device (ppm), MW is the molecular weight of the compound being measured, P is the absolute pressure (atm), R is the ideal gas law constant (0.08206 atm-L/gmol-K), and T is the temperature (K).

The horizontal and vertical dispersion coefficients were determined by Equations 9 and 10, respectively (Cooper and Alley, 2002).

$$\sigma_y = a \cdot X^b \quad (9)$$

$$\sigma_z = c \cdot X^d + f \quad (10)$$

Where X is the distance from the line source to the point of measurement parallel to the wind direction, and the remaining variables (a, b, c, d, f) are constants regulated by the atmospheric stability class at the time of measurement (Turner, 1970). The atmospheric stability class was determined by the solar radiation and wind velocity as described by the EPA's Meteorological Monitoring Guidelines for Regulatory Modeling

Applications (EPA, 2000). The emission factor (EF), given in terms of kilogram of compound per animal per year, was determined using Equation 11.

$$EF = \frac{ER \cdot A \cdot 3600 \cdot 24 \cdot 365}{SD \cdot 10^9} \quad (11)$$

Where EF is the emission factor for the area source (kg/hd-year), A is the area of the source (m^2), and SD is the stocking density of the cattle (m^2/hd).

Non-Flow-Through Non-Steady-State Chambers

NFT-NSS chamber measurements are performed by anchoring a chamber of known area to the soil of an area source of interest. At least four samples of head space gas are removed with use of a syringe over a specific time period, usually a maximum of thirty minutes, and analyzed using gas chromatography to determine concentrations. There are two ways of assuming the analyte concentration relationship to time in the chamber headspace, a linear or curve-linear relationship (Parkin and Venterea, 2010). A curve-linear relationship was assumed for this evaluation, which allows a regression of concentration versus time to be applied. The trace gas flux is defined by the first derivative of the quadratic equation at time zero that fits the concentration versus time (Figure 3).

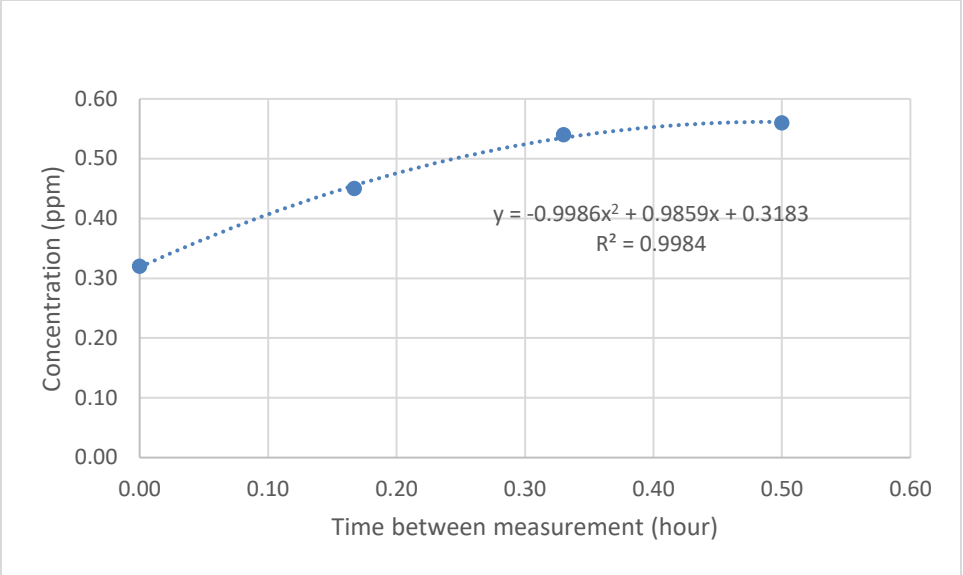

Figure 3. Example of regression used to determine gas emission rate from NFR-NSS chamber measurements.

Flow-Through Steady-State Chambers

FT-SS chamber measurements are performed by placing a chamber of known area on the surface of an area source in question (Borhan et al., 2011). Four holes are required in the top of the chamber, three evenly spaced around the perimeter, and one at the apex of the chamber (Figure 4).

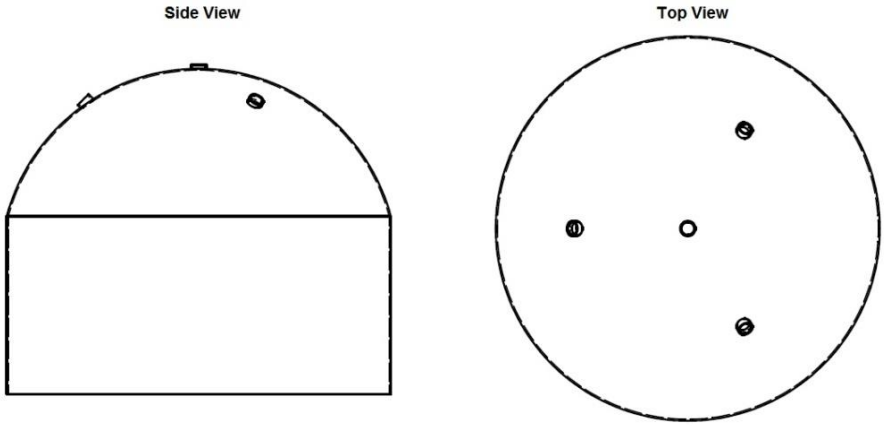

Figure 4. Diagram of a FT-SS chamber.

A vacuum pump is connected to the hole at the apex to draw sample air at a flow rate of 2 L/min to a gas chromatograph for analysis. One of the holes around the circumference of the lid is used to feed sweep gas, contaminant free, at a flow rate of 5 L/min into the chamber. The other two holes allow sweep gas to vent from the FT-SS chamber to avoid a pressurized environment and limit the potential to create a microenvironment during sampling (Figure 5).

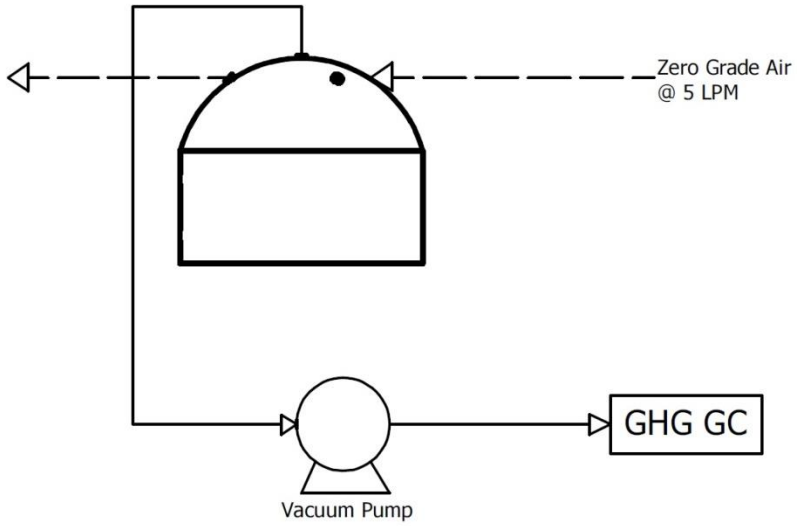

Figure 5. Diagram demonstrating the setup of a FT-SS chamber.

Sweep gas flows through the system for thirty minutes prior to sampling and continues during sampling. The emission flux (Eflux) (micrograms per square meter per minute (μg/m^2-min)) and emission factor (EF) (kilograms of compound per animal per year (kg/hd-year)) are determined by Equations 12 and 13, respectively (Borhan et al., 2011).

$$\text{Eflux} = \frac{C_{mass} \cdot Q}{A_{fc}} \tag{12}$$

$$\text{EF} = \frac{\text{Eflux} \cdot 60 \cdot 24 \cdot 365 \cdot SD}{10^9} \tag{13}$$

Where C_{mass} is the mass concentration of the compound measured (μg/m^3), Q is the supplied flow rate of air to the flux chamber (m^3/min), and SD is the stocking density of the cattle (m^2/hd).

NFT-NSS and FT-SS chambers have the advantages of producing an emission rate without the use of reverse air dispersion modeling and the ability to measure an isolated portion of a large area source. Characterization of spatial variability in emissions is possible by measuring isolated portions of a large area source. The FT-SS chamber method has the advantage of field analysis with the use of a portable gas chromatograph eliminating the risk of sample adulteration during transportation to a lab. NFT-NSS chamber samples have a waiting period between the time of sample collection and analysis. This waiting period allows for potential reactions of compounds and leakage of the sample to occur before analysis. Disadvantages of both chamber methods are the creation of microenvironments inside the chambers and the high cost of individual measurements. In order to account for the spatial heterogeneity of large area sources, numerous flux chamber measurements spaced randomly throughout the area source are required. The numerous measurements lead to a large commitment of labor and time to collect reliable and representative data.

Primary Measurements

Data used to determine total systematic uncertainty for each method were provided from a series of onsite experiments conducted at a feed yard in the high plains of Texas (Figure 6). Concentration data for the source-integrated methods were supplied by onsite measurement using a bistatic OP-FTIR system on the downwind side of the feed yard (Figure 6). Meteorological data were measured onsite using a weather station erected 5 meters to the north of the OP-FTIR path. The weather station measured relative

humidity, air temperature, wind speed and direction, barometric pressure, precipitation, and solar radiation. Representative concentration data for the source-specific methods were taken at the feed yard and provided by Dr. Saidul Borhan (Borhan et al., 2011) and Dr. Ken Casey (Ken Casey, Texas A&M Agrilife Research, personal communications, July 27, 2011) for FT-SS and NFT-NSS chambers, respectively.

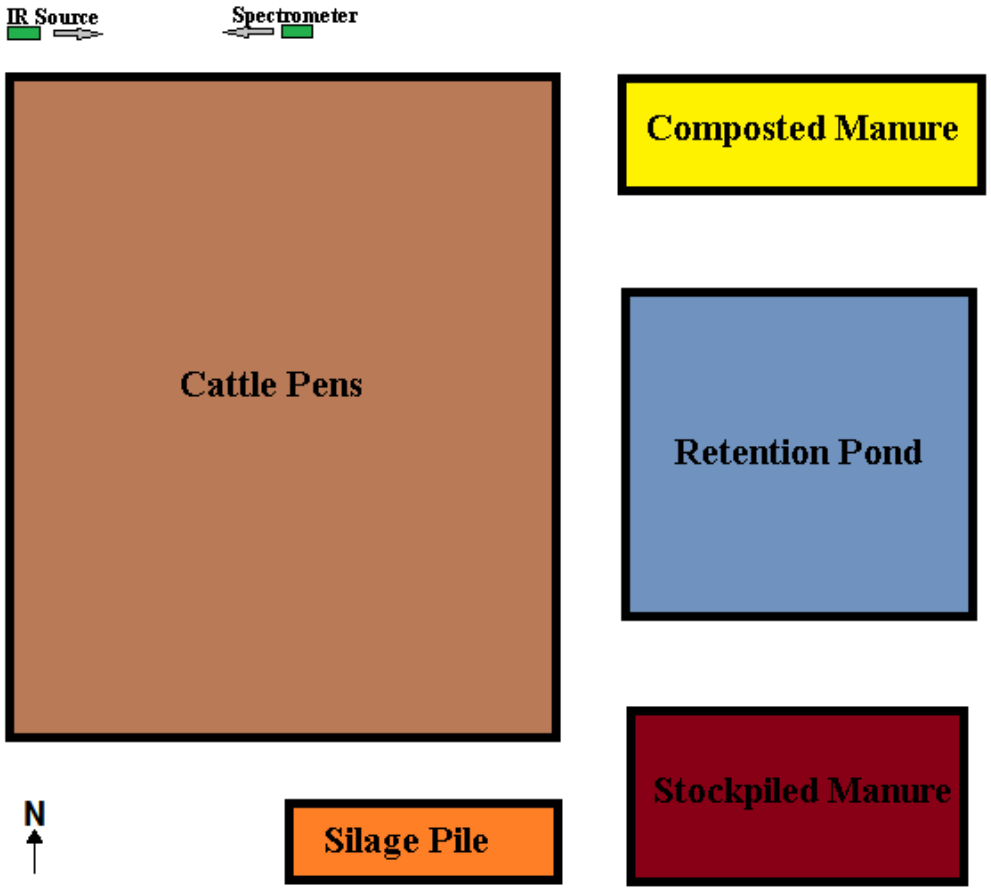

Figure 6. Block figure demonstrating the layout of the large area source and the position of the OP-FTIR system. The cattle pens were 1130 m by 825 m with feed lanes running east to west.

Each measurement method is dependent on different primary variables (i.e. the variables directly measured). The primary variables and their respective uncertainties are listed in Table 2 for the source-integrated methods and Table 3 for source-specific methods. The uncertainty analysis was conducted with a range of values for most of the primary variables as described in Table 4. Comparable equipment accuracy for measuring common primary variables (e.g., injection volumes into the gas chromatograph) were assumed between similar methods to eliminate bias in calculated uncertainties resulting from different primary measurement methods.

Table 2. Primary measurement errors for source-integrated methods.

Primary Measurements	Monostatic OP-FTIR	Bistatic OP-FTIR	OP-TDLAS[b,c]
N_2O Concentration (ppm)	0.0071 – 0.0516[a]	0.0047 – 0.0344[a]	N/A
CH_4 Concentration (ppm)	0.0477 – 0.7836[a]	0.0318 – 0.5224[a]	0.007
Wind Velocity (m/s)[d]	0.05	0.05	0.05
Vertical Dispersion Coefficient (%)	20%	20%	20%
Horizontal Dispersion Coefficient (%)	20%	20%	20%
Temperature (K)[e]	0.6	0.6	0.6
Barometric Pressure (atm)[f]	1.46E-3	1.46E-3	1.46E-3

[a] The uncertainty varies with each measurement relative to the fit of reference spectra to measured spectra within the specified wave regions.
[b] N_2O measurement is unreliable with OP-TDLAS because of potential interference with CO_2 and H_2O absorbance bands.
[c] Gasfinder 2.0 (Boreal Laser, Edmonton, Alberta)
[d] Model 81000 Ultrasonic Anemometer (R M Young Company, Traverse City, Michigan)
[e] HMP60-L Temperature and Relative Humidity Probe (Campbell Scientific, Logan, Utah)
[f] CS100 Barometric pressure sensor (Campbell Scientific, Logan, Utah)

Table 3. Primary measurement errors for source-specific methods.

Primary Measurements	NFT-NSS Chamber	FT-SS Chamber
Chamber Dimension (mm)[a]	1	1
Volumetric Flow Rate[b]	n/a	± 0.8% Reading, ± 0.2% Full Scale
Concentration	CH_4 = 31 ppb, N_2O = 12 ppb[c]	2%[d]
Temperature (K)[e]	0.6	0.6
Barometric Pressure (atm)[f]	1.46E-3	1.46E-3

[a] Chamber dimension refers to chamber base height and diameter of the NFT-NSS chamber and chamber base diameter of the FT-SS chamber.
[b] Model EW-32908-69 Mass and Volumetric Flow meter (Cole-Parmer, Vernon Hills, Illinois)
[c] Varian 450-GC (Varian, Santa Clara, California)
[d] Model 8610C Gas Chromatograph (SRI Instruments, Menlo Park, California)
[e] HMP60-L Temperature and Relative Humidity Probe (Campbell Scientific, Logan, Utah)
[f] CS100 Barometric pressure sensor (Campbell Scientific, Logan, Utah)

Table 4. Range of primary variable values used in uncertainty analysis.

Primary Measurements	Source-integrated	NFT-NSS	FT-SS
N_2O Concentration (ppm)	0.151 – 0.537	0.310 – 2.37	0.069 – 1.74
CH_4 Concentration (ppm)	1.19 – 8.77	2.01 – 47.07	0.627 – 27.91
Wind Velocity (m/s)	0.02 – 18.36	N/A	N/A
Temperature (K)	263 - 310	296 – 310	298
Barometric Pressure (atm)	0.863 – 0.900	0.879 – 0.884	1

Temperature and barometric pressure were used to adjust measured concentrations for air density. Wind speed and direction were used in reverse air dispersion modeling for source-integrated methods to determine source emission rates from the downwind concentration measurement (Harper et al., 2009). In this study a Gaussian model as described by Cooper and Alley (2002) was used for the reverse air dispersion modeling.

The uncertainty of concentration for the OP-FTIR systems was determined for each measurement during analysis and varied based on the fit of reference spectra to the measured spectra being analyzed. The concentration uncertainty for OP-TDLAS was assumed to be similar to the uncertainty in concentrations observed when using a Gasfinder 2.0, 0.007 ppm (Boreal Laser, Edmonton, Alberta). Uncertainties in wind speed and direction were assumed to be similar to those encountered when using of a Model 81000 Ultrasonic Anemometer, 0.05 m/s and 2 degrees (R M Young Company, Traverse City, Michigan).

The dimension of the chambers for both NFT-NSS and FT-SS methods was assumed to be within 1 mm. As described by Borhan et al. (2011), volumetric flow rate of the FT-SS method was monitored and maintained by a Model EW-32908-69 Mass and Volumetric Flow Controller manufactured by Cole-Parmer. The mass flow controller has an accuracy of 0.8% of the reading or 0.01 L/min; the larger of the two was used for the estimation of total systematic uncertainty (Cole-Parmer, Vernon Hills, Illinois). Gas concentrations were determined for the FT-SS method using a Model 8610C gas chromatograph (GC) manufactured by SRI instruments (SRI Instruments, Menlo Park, California). The 2% uncertainty for the GC is based on calibration of the specific GC and is considered conservative (i.e., large) when compared to other GC instruments. Gas concentrations were determined for the NFT-NSS method using a Varian 450 gas chromatograph (GC) manufactured by Varian, Inc. (Varian, Santa Clara, California). The 31 ppb and 12 ppb uncertainties for CH_4 and N_2O, respectively, represented for the GC is based on calibration performed by Dr. Ken Casey

(Ken Casey, Texas A&M Agrilife Research, personal communications, May 29, 2013) of the specific GC. Both GCs used to measure concentrations for the source-specific methods were equipped with a flame ionization detector (FID) for CH_4 detection and an electron capture detector (ECD) for N_2O detection.

Results and Discussion

The Taylor series uncertainty analysis produced a normal distribution of total systematic uncertainties when calculating emission factors for each method. Subsequently, the total systematic uncertainties reported in Table 5 are the average values. The contributions to the total systematic uncertainty are reported as a median.

Table 5. Average systematic uncertainty in emission factor calculation for source-integrated methods and median values of the primary measurement contributions.

Primary Measurements	CH_4			N_2O	
	Monostatic OP-FTIR	Bistatic OP-FTIR	OP-TDLAS	Monostatic OP-FTIR	Bistatic OP-FTIR
Total Systematic Uncertainty	15.16% (43.28%)	15.16% (43.28%)	15.16% (43.28%)	15.16% (44.92%)	15.16% (44.92%)
Contributions to Total Systematic Uncertainty					
Concentration	3.29%	1.58%	0.01%	3.78%	1.85%
Wind Velocity	4.04%	4.19%	2.72%	3.94%	4.12%
Vertical Dispersion Coefficient	92.66%	94.22%	97.27%	92.17%	93.91%
Horizontal Dispersion Coefficient	< 0.01%	< 0.01%	< 0.01%	0.11%	0.12%
Temperature	< 0.01%	< 0.01%	0.01%	< 0.01%	< 0.01%
Barometric Pressure	< 0.01%	< 0.01%	< 0.01%	< 0.01%	< 0.01%

[a] Values reported in parenthesis take into account the uncertainty from averaging all measurements to overcome temporal heterogeneity of the large area source.

The source-integrated methods had an average uncertainty of 15.2% for CH_4 and N_2O when determining an emission factor. The OP-TDLAS is not well suited for measuring N_2O because of interferences with the spectra for water vapor and CO_2 (Soleyn, 2009), therefore the OP-TDLAS was not evaluated for N_2O. The uncertainty did not vary between the source-integrated methods because of the dominance in uncertainty from the reverse air dispersion modeling required to determine an emission rate. Uncertainty in the vertical dispersion coefficient, required by the reverse air dispersion modeling, accounted for greater than 90% of the uncertainty for all source-integrate methods. The uncertainty from the vertical dispersion coefficient could be reduced by using the radial plume mapping method with a monostatic OP-FTIR system. However,

the radial plume mapping method would not be capable of evaluating the full extent of a very large plume (e.g. 1 km wide plume) because of path length restrictions of a monostatic system compared to a bistatic system (Hashmonay, 2008). While OP-TDLAS systems cost less than OP-FTIR systems, they are specifically designed to measure one to three compounds and are not well suited for measuring N_2O, limiting the potential applications of the OP-TDLAS system relative to either of the OP-FTIR methods. The decreased uncertainty in concentration detection with the OP-TDLAS over the OP-FTIR methods, results in an increased relative contribution of the other primary variables, such as wind velocity and vertical dispersion coefficient.

The bistatic OP-FTIR method has a lower concentration uncertainty than the monostatic OP-FTIR method regardless of compound measured because of an increase in number of reflective optics required by a monostatic system compared to a bistatic system. In addition to the optical mirrors required to focus the IR signal for the spectrometer (required for both systems), the monostatic system requires an optical mirror (i.e., the retroreflector) at the end of the path to reflect the IR signal back towards the spectrometer. The bistatic system does not require this additional optical mirror because the IR source is aligned directly with the spectrometer. In other words, the monostatic system has a double-pass path, while the bistatic system implements a direct path. The increased number of reflective optics leads to a decrease in signal strength for the monostatic system compared to a bistatic system with an identical path length. For this same reason the wind velocity and vertical dispersion coefficient contributes a greater

percentage of the total systematic uncertainty when determining emission factors with bistatic system than with a monostatic system.

Measurement with a single FT-SS chamber presented a lower total systematic uncertainty (Table 6) than source-integrated methods (Table 5) and NFT-NSS chamber. The total systematic uncertainty is lower for a single FT-SS compared to source-integrated methods because reverse air dispersion modeling is not required. Single measurement with NFT-NSS chambers show a higher systematic uncertainty than FT-SS chambers because of the regression used to determine the emission rate from the NFT-NSS chamber. However, both source-specific methods are limited by the large number of samples required to assure a representative sample has been acquired to account for spatial heterogeneity. The total systematic uncertainty increased to 75.9% and 84.96% for the NFT-NSS method and 87.6% and 53.0% for the FT-SS method when measuring CH_4 and N_2O, respectively, after averaging the emission factors calculated from each sample. Assuming the samples collected by the flux chambers are representative of the population, it would take approximately 1500 samples for CH_4 and N_2O to match the 15.2% uncertainty of source-integrated methods.

Table 6. Average total systematic uncertainty in emission factor calculation for source-specific methods and median values of the primary measurement contributions.

Primary Measurements	CH_4		N_2O	
	NFT-NSS Chamber	FT-SS Chamber	NFT-NSS Chamber	FT-SS Chamber
Total Systematic Uncertainty[a]	21.23% (75.93%)	13.51% (87.56%)	24.59% (84.96%)	13.51% (52.99%)
Contributions to Total Systematic Uncertainty				
Chamber Dimension	< 0.01%	< 0.01%	< 0.01%	< 0.01%
Volumetric Flow Rate	--	0.01%	--	0.01%
Concentration	99.99%	98.47%	99.99%	98.47%
Temperature	< 0.01%	1.00%	< 0.01%	1.00%
Barometric Pressure	< 0.01%	0.52%	< 0.01%	0.52%

[a] Values reported in parenthesis take into account the uncertainty from averaging all flux chamber measurements to overcome spatial heterogeneity of the large area source.

Table 7 details the average emission factor measured, the standard deviation of the measurements and the number of measurements by each measurement method when measuring CH_4. Table 8 details the same information for each measurement method when measuring N_2O.

Table 7. Summary of results for each measurement method when measuring CH_4.

	Bistatic OP-FTIR	Monostatic OP-FTIR	OP-TDLAS	NFT-NSS Chamber	FT-SS Chamber
Average Emission Factor (kg/hd-yr)	68.52	68.52	68.52	0.36	0.52
Number of Measurements	52,929	52,929	52,929	110	153
Standard Deviation of Emission Factors	29.66	29.66	29.66	0.27	0.45

Table 8. Summary of results for each measurement method when measuring N_2O.

	Bistatic OP-FTIR	Monostatic OP-FTIR	OP-TDLAS	NFT-NSS Chamber	FT-SS Chamber
Average Emission Factor (kg/hd-yr)	7.56	7.56	7.56	0.05	0.13
Number of Measurements	52,929	52,929	52,929	152	167
Standard Deviation of Emission Factors	3.40	3.40	3.40	0.04	0.07

Conclusion

Based on the results of this study, NFT-NSS and FT-SS chamber emission rates were characterized by comparable systematic uncertainties in emission factor determination for both CH_4 and N_2O measurements. The source-specific methods require much more labor compared to source-integrated methods because of the requirement that a large number of samples be collected to overcome the spatial heterogeneity of large area

sources. After averaging the emission factors calculated from each sample to account for spatial heterogeneity, the total systematic uncertainty increased to 75.9% and 84.96% for the NFT-NSS method and 87.6% and 53.0% for the FT-SS method when measuring CH_4 and N_2O, respectively. This increase is because of the variation in concentration measured by each sample.

Source-integrated sampling techniques have an average systematic uncertainty of 15.2% when measuring CH_4 and N_2O because of the dominance of the air dispersion modeling required by each method to determine an emission rate. Specifically, the uncertainty in vertical dispersion as part of the air dispersion modeling dominates the uncertainty of the source-integrated methods. The uncertainty from the vertical dispersion coefficient could be reduced by utilizing the radial plume method with a monostatic FTIR system. OP-TDLAS is limited by the reduced number of compounds it is capable of detecting (including N_2O), but it is the least costly of the source-integrated methods and measures CH_4 more precisely than FTIR methods. OP-FTIR systems are capable of measuring concentrations in real time, much like the OP-TDLAS, but are capable of measuring a vast array of compounds without the requirement of reference gases.

When source-specific and source-integrated methods are used simultaneously it is possible to more accurately determine emission factors than if either were used on their own. Source-specific methods are capable of individually characterizing the multiple sources of GHGs present in a large area source, while source-integrated methods can account for the temporal and spatially heterogeneous aspect of large area sources.

CHAPTER III

GREENHOUSE GAS MEASUREMENT FROM A GROUND-LEVEL AREA SOURCE WITH OP-FTIR

Introduction

In December 2009, the EPA's Mandatory Reporting of Greenhouse Gases Final Rule (MRR) took effect, which requires reporting of greenhouse gas (GHG) emissions from facilities emitting 25,000 metric tons of carbon dioxide equivalents (CO_2e) per year (FR 74 at 56373). A CO_2e is defined as a compound's global warming potential (GWP) compared to carbon dioxide (CO_2). The purpose of the rule is "to collect accurate and timely GHG information for future regulation and policy decisions" (FR 74 at 56373). Emissions from manure management at cattle operations emitting more than 25,000 metric tons CO_2e per year are subject to the rule under Subpart JJ. Emissions resulting from enteric fermentation are not subject to reporting requirements because practical methods to estimate enteric fermentation emissions are difficult to implement and fraught with uncertainty (FR 74 at 56373).

The MRR is of concern to the feed yard industry because of greater concentrated mass of manure to manage as compared to other agricultural industries (Eghball and Power, 1994). According to the Intergovernmental Panel on Climate Change (IPCC) the enhanced global beef demand will cause increased emissions of methane (CH_4) and nitrous oxide (N_2O) from amplified beef cattle herd size, while the use of nitrogen fertilizer

in North America has stabilized causing the contribution of GHG emissions from crops to be stagnant. This leaves the main increase of agricultural GHG emissions to management practices of cattle, poultry, and swine manure (IPCC, 2007). Methane (CH_4) and N_2O have CO_2e of 21 and 310, respectively, meaning that one ton of CH_4 has 21 times the global warming potential of one ton of CO_2 emissions (FR 74 at 56373).

According to the current rule, agricultural emissions are estimated using IPCC emission factors which have been determined to have uncertainties of ±30% to ±50% (Eggleston et al., 2006). These emission factors were established in the 1990's with methods and equipment that are less precise than modern instrumentation and based on research performed in multiple countries such that the emission factors may not represent modern US production and management practices. If accurate emission factors representative of modern US agricultural production practices are not correctly identified, future regulation of emitting operations may be based on inaccurate or biased emissions estimates.

Quantifying GHG emissions from agricultural ground-level area sources such as feed yard operations is challenging because of the temporal and spatial heterogeneity of emissions. At a feed yard operation, many diverse sources of GHGs are located in an expansive open environment, making it costly and difficult to accurately characterize emissions from any one specific source. The generation of GHGs from manure management is dependent on many factors including surface temperature, pH, carbon-to-nitrogen and water-to-solids ratios, nutrient composition, particle size, retention time and

more which makes it difficult to develop a reliable emission factor for an ever-changing environment (Weiske et al., 2005).

A study was conducted from May 2010 to November 2011 to evaluate the use of a bistatic open-path Fourier Transform Infrared Spectroscopy (OP-FTIR) system to measure CH_4 and N_2O from a feed yard in the High Plains of Texas. For this study, emissions were characterized using alternating upwind and downwind concentrations supplied by a single OP-FTIR system. Ideally, two spectrometers would be used, one upwind and one downwind of the area under evaluation for differential concentration measurement, but this was a "proof of concept" study to determine requirements and data quality to assess the desirability of investing in another OP-FTIR system. The objective of this study was to identify the short comings of using an OP-FTIR system to characterize GHG emissions from a large area source, develop operational guidelines for such a system, maintenance requirements, quality of data, and explore the practicality of using a single measurement system to identify emission trends.

OP-FTIR systems have been deployed in a range of research studies pertaining to large area sources with a focus of measuring multiple compounds. Table 9 lists some of these previous studies and a brief description of the area source evaluated.

Table 9. Previous studies involving the use of an OP-FTIR to characterize a large area source.

Reference	Compound Measured	Ground-level Area Source Evaluated
Reese et al., 2009	NH_3	Waste treatment lagoon at a 6000-cow dairy in Idaho & 950-milking cow dairy in central California
Kirchgessner et al., 1993	CH_4	Caballo coal mine in the Powder River region of Wyoming
Shores et al., 2005	NH_3, CH_4	Anaerobic lagoon at a 980-head swine farm in eastern North Carolina
Bjorneberg et al., 2009	NH_3, CH_4, N_2O	700-cow dairy farm in southern Idaho

Methods

Experimental Setup

The experiment was conducted at a feed yard in the high plains of Texas with a potential maximum capacity of 50,000 head of cattle. The feed yard was partitioned into multiple CH_4 and N_2O that included enteric fermentation from the cattle, the manure in the pens, silage storage, manure storage, and a storage lagoon for runoff water from the pens. The goal of this experiment was to characterize CH_4 and N_2O emissions from the hypothesized largest emission source of GHGs, the cattle pens. A single bistatic OP-FTIR system was initially placed 27 m north and parallel to the cattle pens such that the full east to west extent of the cattle pens' plume would be encompassed by the path of the measurement system (Figure 7) during a southern wind. The north side was chosen for placement because the predominant wind direction in the area is from the south (Figure 8).

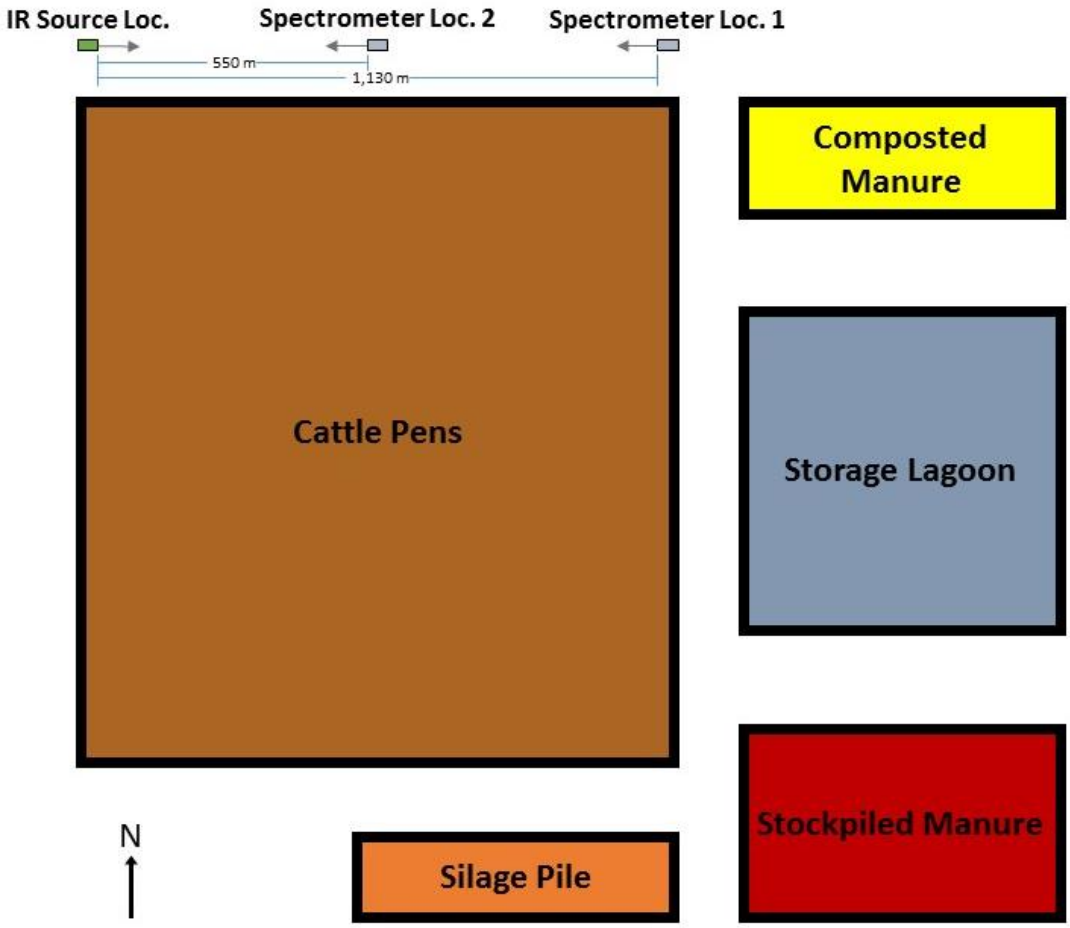

Figure 7. Block figure demonstrating the layout of the area source and the initial (Spectrometer Loc. 1) and final (Spectrometer Loc. 2) positions of the OP-FTIR system. The cattle pens were 1,130 m by 825 m with feed lanes running east to west.

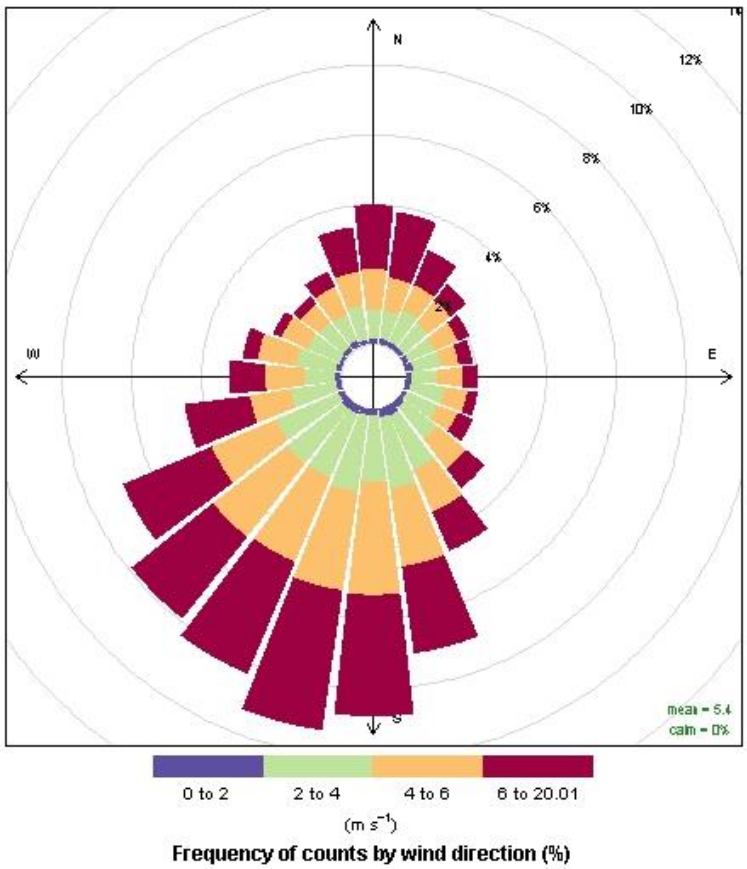

Figure 8. Wind rose characterizing the wind at the feed yard during the span of the study.

Bistatic OP-FTIR systems consist of two pieces of equipment, an infrared (IR) source and spectrometer. The IR source and spectrometer were positioned north of the northwest and northeast corners of the cattle pens, respectively. Given the Gaussian dispersion of emissions, the OP-FTIR was initially placed near the source to minimize the influence from outside sources, as discussed by Faulkner et al. (2007). Measurements were conducted along the line of maximum concentration (LMC) relative to the prevailing wind to limit modeling uncertainty from dispersion parameter uncertainties near the edge of the plume (Faulkner et al., 2007). As shown in Figure 9 (Faulkner et al., 2007), the

LMC is oriented perpendicular to the wind direction and downwind of the source, and it shortens with increasing distance from the source to account for the Gaussian uncertainties at the edges of the plume. The uncertainty at the edges of the plume is a function of the vertical spread parameter of the plume (Turner, 1970), which is represented as σ_y. The only measurements of interest were along the LMC, thereby limiting the evaluation to periods that were most influenced by the source of interest. More characteristic emission rate estimates can be achieved by ignoring measurements outside of the LMC of the emission source in question (Wanjura et al., 2004).

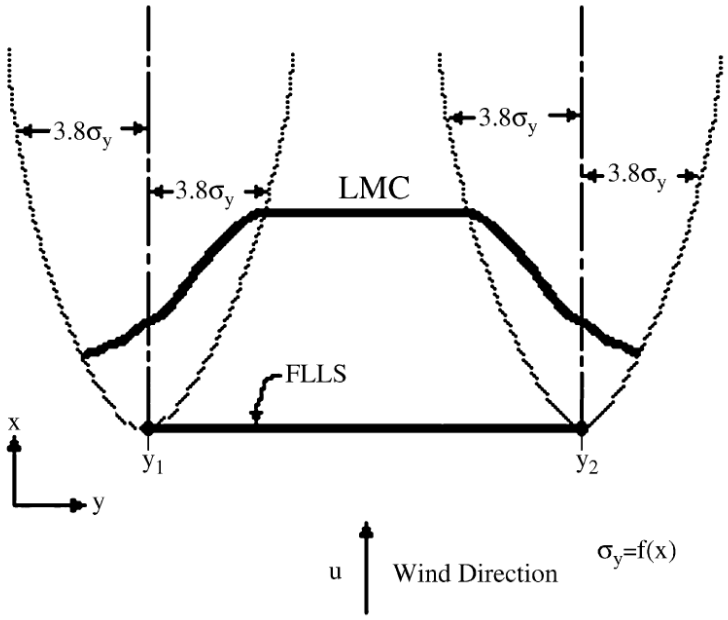

Figure 9. Graphical representation of the line of maximum concentration with respect to a large area source. From Faulkner et al. (2007).

The original placement of the OP-FTIR system resulted in a path length of 1,130 meters. This path length was used initially based on the concept that longer the path length the greater the sensitivity in concentration measurements (MIDAC, 2008). After initial deployment, it was determined reliable measurements could not be acquired because of low IR transmittance between the IR source and spectrometer caused by high particulate matter concentrations and consistent loss of alignment between the two devices. Alignment was easily interrupted by the large wind force present in the region and the drastic effect that a small alignment change would have on the signal with such a large path length. To remedy this, the path length was reduced to 550 m by moving the spectrometer closer to the emission source (Figure 7).

Adjusting the path length reduced the issue with IR interference from particulate matter, but alignment was still difficult to maintain. An attempt was made to create a system of linear actuators and cameras to allow for remote alignment of the IR source and spectrometer. Minimal capital was used for the linear actuator system resulting in inconsistent positioning of the linear actuators and poor alignment of the IR source and spectrometer. The alignment issue was eventually remedied with better anchoring of the IR source and spectrometer. It would have been preferred to move both the IR source and spectrometer such that the measurement path was centered east to west with the cattle pens. However, the IR source could not be relocated any further from the original location because of limited availability of power sources.

Preferably, A measurement system would be placed upwind and another downwind from the emission source to reliably measure downwind impacts from the area source. The use of two systems would produce a differential concentration isolating the contribution from the emission source in question from the native background concentration and other emission sources in the area. This was a proof of concept experiment where the OP-FTIR technology was under evaluation; therefore, a second OP-FTIR system was not used. The upwind measurement was assumed to be the background concentrations (i.e. ambient for the surrounding area) and constant throughout the measurement period. Any increases in concentrations in the downwind measurement were assumed to originate from the feed yard. The current background concentration of N_2O in the atmosphere is 310 ppb (Kawashima et al., 1996) and CH_4 has been measured as 1.829 ppm ±0.175 (Todd et al., 2010). Other potential sources of CH_4 and N_2O in the area include the composted and stockpiled manure to the northeast and southeast of the cattle pens, the storage lagoon to the east of the cattle pens where run off water from the cattle pens is stored, and the silage pit to the south of the cattle pens. The prevailing wind is from the south, therefore, the single system purchased was placed north of the emission source to collect the greatest number of downwind measurements possible with a single system.

Meteorological data were supplied by a weather station erected 5 meters to the north of the OP-FTIR path (Figure 10). The weather station measured temperature, relative humidity, barometric pressure, precipitation, solar radiation, and wind speed and direction. These data are necessary for reverse air dispersion modeling to determine

emission rates from the area source and to identify trends in CH_4 and N_2O concentrations compared to meteorological variables.

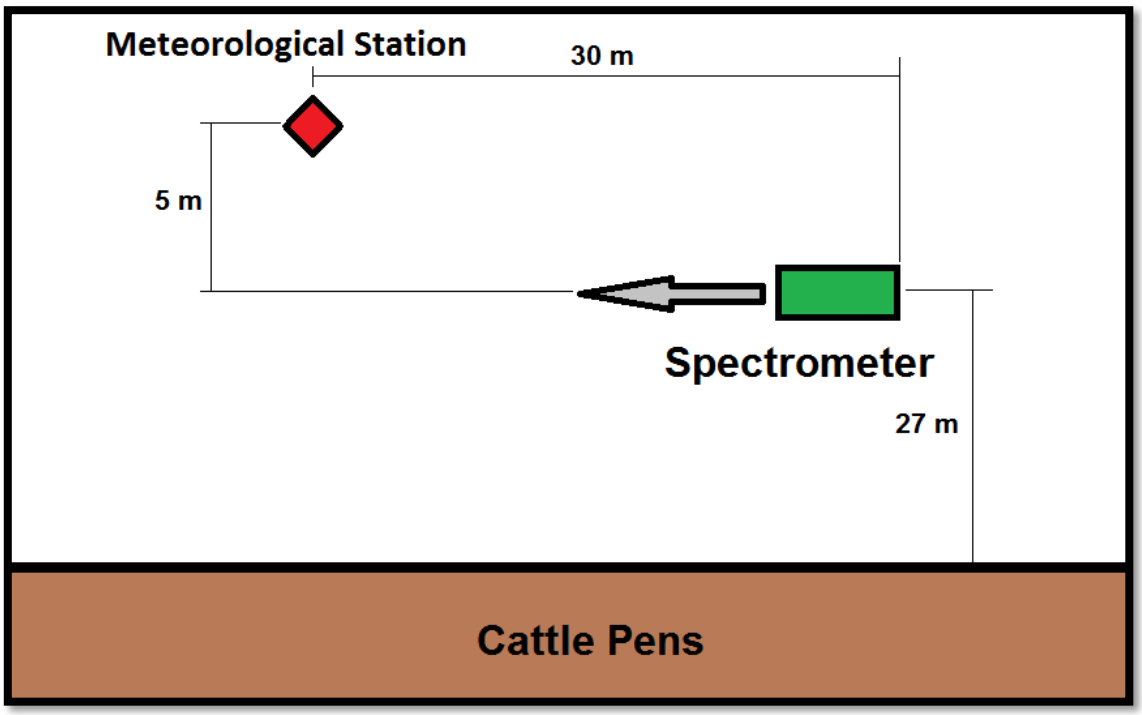

Figure 10. Block figure demonstrating the layout of the OP-FTIR system and meteorological station with respect to the area source.

Equipment

An OP-FTIR system utilizes an IR beam directed toward a spectrometer to measure concentrations of multiple gases simultaneously. Between the source of the IR beam and spectrometer, compounds in the air absorb a portion of the IR signal at specific wavenumbers respective to the compounds present. The spectrometer quantifies the absorbance of IR energy based on the presence of the compounds which are compared to

reference spectra to determine concentrations of specific compounds in the IR path. The advantage of an OP-FTIR system is the capability of measuring multiple compounds simultaneously through an accurate, non-invasive process (MIDAC, 2008).

There are two types of OP-FTIR systems, a monostatic and bistatic system. A monostatic OP-FTIR system consists of a spectrometer and IR source combined into a single unit. This unit is aligned with a retroreflector to reflect the IR signal created by the source back to the spectrometer. The two instruments are aligned such that the plume from the area source passes through the IR path. In a monostatic OP-FTIR system the IR beam is reflected over the path length a second time before reaching the spectrometer for analysis. This property of the monostatic system decreases the measured path length by at least half. A limited path length can be an issue when evaluating an area source with a wide plume, such as a feed yard. The bistatic OP-FTIR system operates much like the monostatic system except the spectrometer and source are two separate units aligned with one another directly rather than using a retroreflector. These changes allow the system to utilize a longer path length than its monostatic counterpart.

An OP-FTIR system produces an absorbance spectrum that can be analyzed to determine the average concentrations of compounds within the path length. To obtain representative measurements it is important to encompass as much of the plume as possible within the path length (ASTM, 2007). Independent of type, OP-FTIR measurement does not require frequent calibration with reference gases. OP-FTIR systems use well maintained databases of reference spectra to compare with collected data to quantify concentrations of compound of interest.

A bistatic OP-FTIR system (Model: M4413-F, MIDAC Corp., Westfield, MA) was used in this study for its capability to provide longer path lengths then a monostatic, as required when evaluating a feed yard. The IR source (Figure 11) and spectrometer were mounted on trailers to allow for extra mobility if the path length required adjustment.

Figure 11. IR source mounted on a trailer and supported by four trailer jacks.

The spectrometer was encased in a cage that prevented theft, and limited direct UV and precipitation from damaging the device (Figure 12).

Figure 12. Spectrometer mounted on a trailer and protected by a cage enclosure.

Both trailers were fitted with a jack on each corner to allow for quick adjustment of angle and height when aligning the IR source with the spectrometer. When rough alignment was obtained, the trailers were secured in place with turnbuckles and anchors (Figure 13).

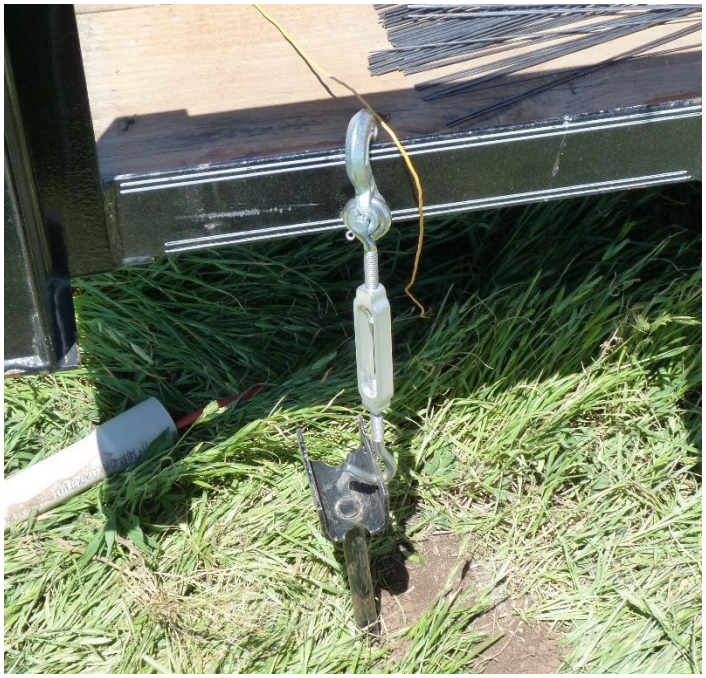

Figure 13. Turnbuckle and anchor system used to secure the trailer in place.

It was later determined that the jacks and anchors were not sufficient to hold the IR source and spectrometer in alignment during the frequent high wind events in the high plains. As a result, four 3-foot-deep concrete piers were put in place for each trailer. In addition, a metal frame was constructed to secure the trailers directly to the piers (Figure 14).

Figure 14. Constructed frame and piers used to secure on side of the trailer holding the spectrometer.

The frame for the IR source had an adjustable screw for vertical alignment and notch system horizontal alignment with the spectrometer (Figure 15). The spectrometer trailer frame did not require a notch system for horizontal adjustment because the spectrometer was mounted on a tripod that allowed for these adjustments.

Figure 15. Adjustable screw used to adjust the angle of the IR source trailer.

The spectrometer was interfaced with a computer by a fiber optic cable. The computer controlled the OP-FTIR system and logged the spectra created by the OP-FTIR with the use of the AutoQuant Pro software (ver. 4.0, MIDAC Corp., Westfield, MA). The OP-FTIR system was operated according to the standard operating procedure included in Appendix A. With the addition of wireless relays (model ZADSSR4xPROXR_XSC, National Control Devices, Osceola, MO) the IR source was operated from the computer terminal instead of requiring project personnel to travel the path length each time the IR source needed to be turned on or off for quality control purposes. The computer was connected to the internet by a Raven XE modem manufactured by Sierra Wireless. The modem allowed trouble shooting and data collection from any computer with an internet connect. The computer and supplemental equipment was housed in an insulated and weather sealed box (Figure 16) on the spectrometer trailer. An air conditioning unit was

installed to cool and circulate the air in the sealed box to prevent the equipment from overheating.

Figure 16. Weather sealed box containing computer and supplemental equipment.

An air compressor and venturri spray nozzle were used to perform cleaning operations of the IR source and spectrometer. The cleaning operations were conducted monthly because particulate matter from the dusty environment would frequently accumulate on the optics of the OP-FTIR system (Appendix B).

Data Analysis

AutoQuant Pro was provided with the OP-FTIR system to operate the system and analyze the spectra collected. A library of reference spectra, compiled by MIDAC Corporation and the EPA, was compared to the collected spectra to determine the

concentration measured for specific compounds. Procedures for conducting this analysis in AutoQuant Pro are provided in Appendix C. These procedures also use the spectral analysis software Essential FTIR (ver. 3.0, Operant LLC, Madison, WI). The open source statistical program R: A Language and Environment for Statistical Computing (ver. 3.2.3, R Development Core Team, 2008) was used in conjunction with the OpenAir package (ver. 1.9, Carslaw and Ropkins, 2012) to identify any trends between measured concentrations and other measured variables.

Results

Methane

Measured CH_4 concentrations during the study are summarized by Table 10. The concentration data are distinguished by upwind and downwind measurements with respect to the emission source.

Table 10. Summary of CH_4 data separated by upwind and downwind measurements.

	Upwind (ppm)	Downwind (ppm)
Maximum	4.97	6.87
Minimum	1.36	1.62
Average	2.18	3.16
Median	2.13	3.04
Standard Deviation	0.37	0.78

Frequency of CH_4 concentration measurements within specified ranges of wind direction are shown in Figure 17. The majority of measurements came from the south, the direction of the area source with respect to the OP-FTIR system. Most measurements greater than 2.5 ppm were from the south. This result shows that the OP-FTIR system was properly positioned to capture the majority of measurements impacted by the feed yard.

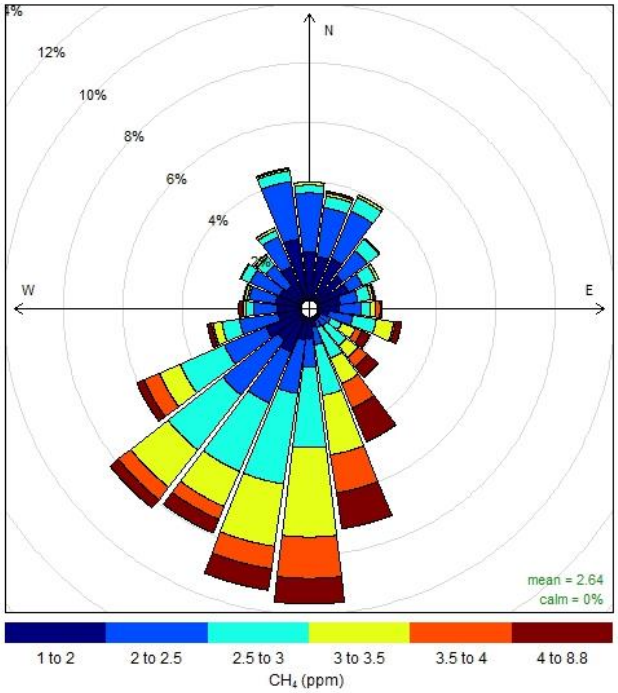

Figure 17. Pollutant rose demonstrating a predominant wind from the south throughout the study, and higher CH_4 concentrations observed when the OP-FTIR system was downwind of the area source.

The mean CH_4 concentration by wind direction and speed is represented in Figure 18. The highest mean concentration is from the southeast direction when the wind was less than 5 m/s. The decrease in concentration with increasing wind speed is possibly from a plume dilution at higher wind speeds caused by a greater flow rate of clean air mixing with the relatively fixed rate of methane emissions from the feed yard. The lowest mean concentration was from the north at the highest measured wind speed. This was of interest because there was another feed yard 11 kilometers (km) to the north of the OP-FTIR system and it was not distinguishable from the background concentration.

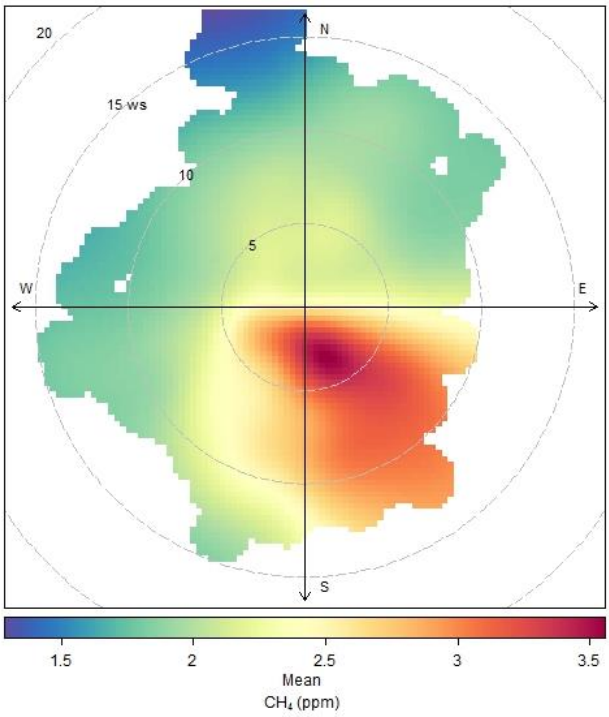

Figure 18. Polar plot presenting mean CH_4 concentration at various wind speeds and directions over the entire period of the study.

Mean methane concentration by wind direction and hour of day is displayed in Figure 19. The highest mean concentration was around midnight possibly from lower temperatures at night time, which allowed for more stable atmospheric conditions that limited plume rise. At higher ambient temperatures during the day time, the warm air rose to cause a mixing effect. This mixing effect diluted the plume leading to lower observed concentrations in the afternoon.

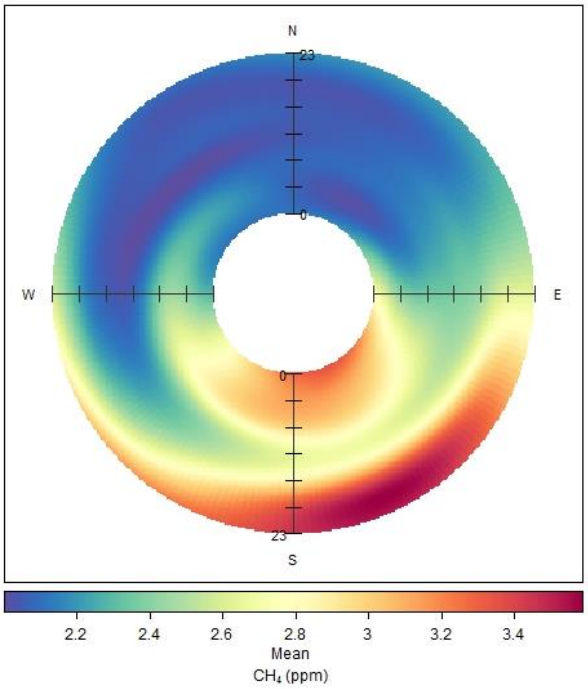

Figure 19. Polar annulus displaying the mean CH_4 concentration by wind direction and hour of day.

A time variation of normalized CH_4 concentration and ambient temperature is shown in Figure 20 for downwind measurements. A diurnal cycle for CH_4 concentration was apparent and corresponds inversely with the change in temperature throughout the day. The same trend was not seen on the month or weekday scale where an increase in temperature correspond to an increase in CH_4 concentration. These observations could be the result of two separate mechanisms, (1) the diurnal trend may be the result from meteorological phenomena that govern the dispersion of a plume, and (2) the increased concentration with temperature on a month scale may be the result of an increase in emission rate at higher temperatures.

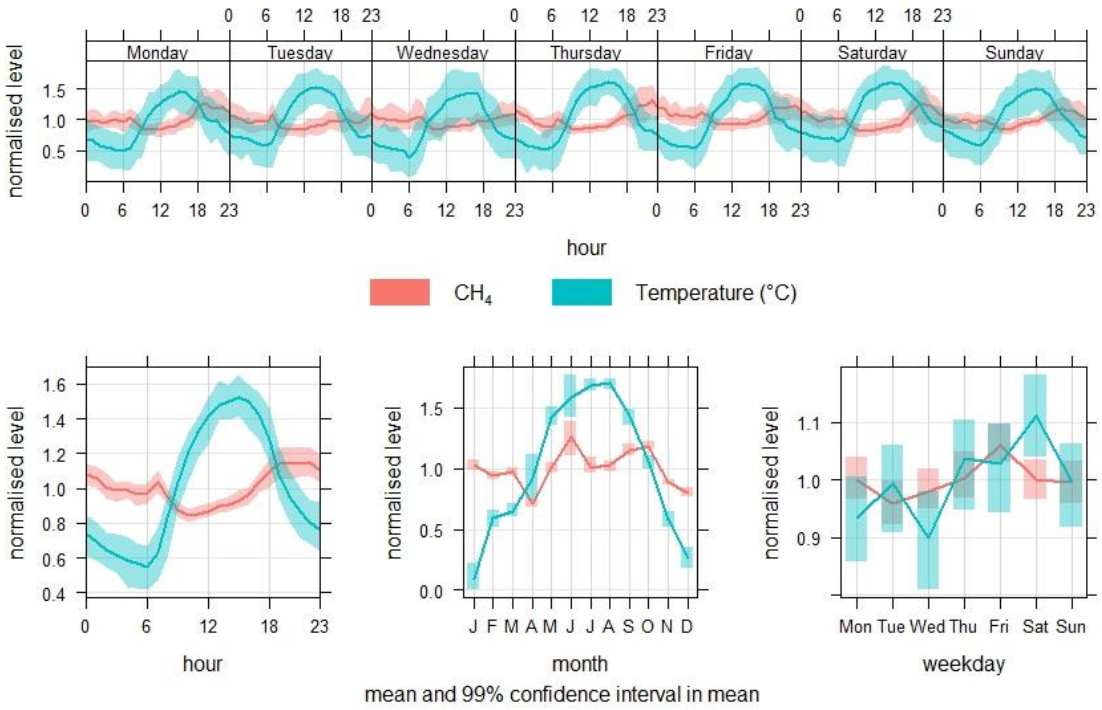

Figure 20. Time variation plot comparing CH_4 concentration and ambient temperature for downwind measurements. A 99% confidence interval is displayed as a shaded area along each line.

A time variation comparison CH_4 concentration when the OP-FTIR system is downwind and upwind of the area source is presented in Figure 21. The upwind measurement was near constant at 2.1 ppm. The 99 percent confidence intervals for upwind and downwind measurements did not overlap; therefore, the upwind measurements could be used as a background concentration on at least a monthly basis with confidence.

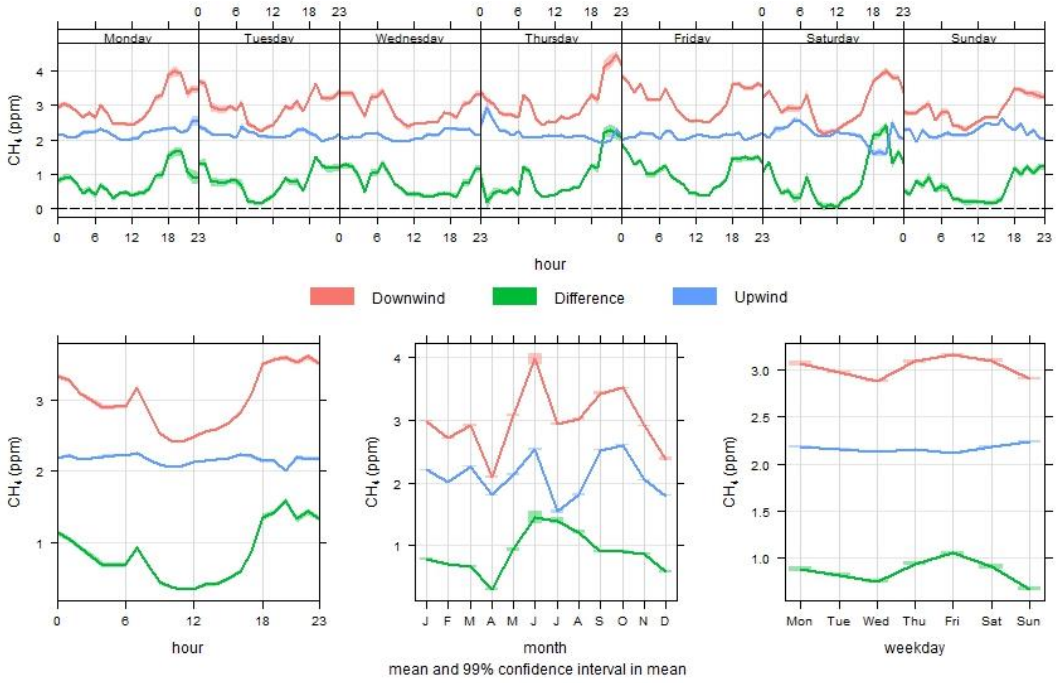

Figure 21. Time variation plot comparing downwind and upwind CH_4 concentration measurements. A 99% confidence interval is displayed as a shaded area along each line.

Nitrous Oxide

Measured N_2O concentrations during the study are summarized by Table 11. The concentration data are distinguished by upwind and downwind measurements with respect to the area source.

Table 11. Summary of N_2O data separated by upwind and downwind measurements.

	Upwind (ppb)	Downwind (ppb)
Maximum	530	514
Minimum	203	168
Average	340	333
Median	334	334
Standard Deviation	52	42

Frequency of N_2O concentration measurements within specified ranges of wind direction is shown in Figure 22. The majority of measurements came from the south, the direction of the area source with respect to the OP-FTIR system. The distribution of concentration by wind direction is consistent. This result shows that either the OP-FTIR system was not measuring N_2O properly, the area source was not a significant source of N_2O compared to the background concentration, or the area was surrounded by significant N_2O sources that drowned out any contribution from the area source.

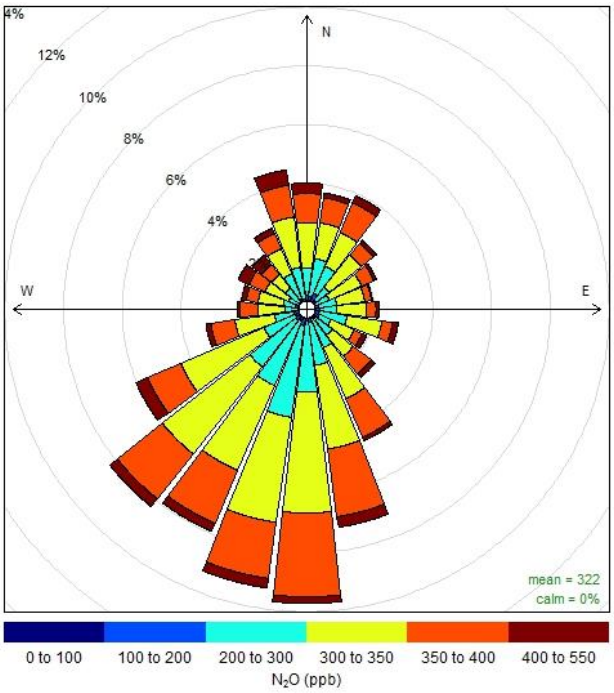

Figure 22. Pollutant rose demonstrating a predominant wind from the south throughout the study, and uniform distribution of N_2O concentration regardless of wind direction.

The mean N_2O concentration by wind direction and speed is represented in Figure 23. There appears to be numerous N_2O sources surrounding the area of study. The greatest contributor to atmospheric N_2O is nitrogen rich fertilizer used by agriculture (IPCC, 2007) and a large portion of the land in the area was fertilized for grain production. With a single OP-FTIR system it was difficult to identify any contribution of N_2O from the area source in the area of study.

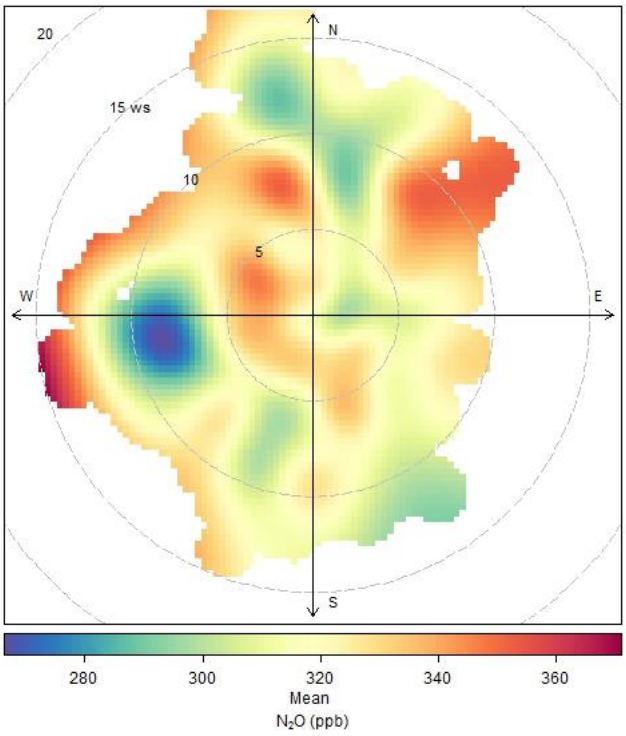

Figure 23. Polar plot presenting mean N_2O concentration at various wind speeds and directions over the entire period of the study.

Discussion

Between May 2010 and November 2011, the OP-FTIR system collected 1,173 hours of reliable measurements. The number of measurements was limited by a number of factors, most of all the frequent system maintenance requirements that could not be met because of the remote location in which the OP-FTIR was deployed. Frequent maintenance was required as a result of the initially underestimated particulate latent environment. It was originally believed that maintenance could be performed on a bi-monthly basis, but it was later determined that a bi-weekly or weekly maintenance regiment would be more appropriate given the dusty environment in which the system was

deployed. An initial hurdle was how to clean the fragile, gold plated optics of the OP-FTIR system. Compressed air was used but proved to be ineffective when cleaning fly excrement from the equipment. This was later remedied with the use of a compressor outfitted with a venturri sprayer attachment to clean the optics with an air and distilled water mixture at pressures no higher than 40 pounds per square inch (psi) (276 kilopascals (kpa)). Cleaning procedures are described in Appendix B.

Another early struggle was with the tripod in which the spectrometer was mounted. The manual adjustment of the tripod did not provide the fine adjustment required to align the spectrometer with the source, and when the tripod was locked into position the spectrometer was still able to move enough to put the spectrometer out of alignment with the IR source. It was determined that a better alternative would be a real-time positioning system with fine degree adjustments.

Mobility of the equipment was believed to be a necessity at the time of the experiment design. This belief became a hindrance when the trailers in which the OP-FTIR system was mounted had enough movement during high winds to cause the system to become misaligned. The movement of the OP-FTIR system during high winds was later remedied by bolting the spectrometer and IR source directly to the metal frame of their respective trailers. The frame of each trailer was then bolted to 3 ft deep concrete piers to ensure stability. The cage that was constructed around the spectrometer proved to be sufficient for its original purpose of preventing theft, but did little to limit airborne dust from fouling the optics. A better solution would have been to retrofit an enclosed trailer rather than a flat trailer. An enclosed trailer would have required much less

fabrication and could have provided a cleaner environment for the equipment. Placing the IR source on a trailer added additional weight and complicated the setup when attempting alignment procedures. A specifically designed structure could have been constructed to easily make these adjustments while reliably securing the source. In contrast to the original experimental design, mobility of the source was not required for a long-term study such as this.

Another issue was the placement of the spectrometer and IR source. These should have been placed such that the measurement path was centered with respect to the area source of interest, the feed yard. This was not possible because of limitation of access to a power source for the IR source.

The OP-FTIR system was capable of measuring multiple compounds simultaneously with great accuracy, and it was hypothesized that a single system would provide an emission estimate within an order of magnitude of the actual emissions. Based on the outcome of the initial evaluation it could be determined whether or not to invest in another OP-FTIR system. Upwind measurements were to be considered background measurements with respect to the downwind measurements. Keeping this concept in mind the OP-FTIR system was placed on the north side of the area source, since the wind in the area predominantly comes from the south, as demonstrated by Figure 8.

The hypothesis that a single system could produce accurate measurements of emissions from a large area source was only valid in situations where a large amount of upwind and downwind data over a given time frame was available and the variance of the upwind background measurements in the data was relatively low. Figure 21 verifies this

hypothesis for CH_4 when applied on a monthly basis. To subtract a background concentration on an hourly basis would still require a second system to place on the opposite side of area source. Another system would be required to differentiate any contribution from the area source to the measured N_2O concentration from the surrounding sources on any time scale.

With another system positioned on the south side of the area source, a background measurement could be procured and subtracted from the downwind measurement to determine a differential concentration from the area source on an hour basis. With this information paired with reverse air dispersion modeling, emission factors could be developed for use with future GHG regulations.

Conclusion

An OP-FTIR system is a viable measurement device for characterizing GHG emissions from a large area source. The range of measured 1-hour average CH_4 concentrations were 1.62-6.87 ppm and 1.36-4.97 ppm for downwind and upwind measurements, respectively. Measured 1-hour average N_2O concentrations were 168-514 ppb and 203-530 ppb for downwind and upwind measurements, respectively. There was not a statistical difference between upwind and downwind measurements for N_2O. This was believed to be from the common use of nitrogen rich fertilizer in the surrounding area for grain production. The additional sources of N_2O drowned out any contributions to the measured concentration from the area source. Two OP-FTIR systems would be required to obtain more refined data for differentiation of the area source from surrounding sources two systems would be required. One OP-FTIR system would be placed downwind and the other upwind of the area source to produce a differential concentration.

With the dusty environment, it would have been preferred to house OP-FTIR system in a modified enclosed trailer with an opening that allowed for direct line of site between the spectrometer and IR source. The manual tripod chosen for this study had too much play when locked to maintain alignment of the spectrometer and IR source during high wind events. In future studies, it is suggested to use a real-time positioning system with fine degree adjustments even though such a system may be costly. Stability of the

spectrometer and IR source should be considered a priority and maintenance should be performed on a weekly or bi-weekly basis to obtain a consistent stream of usable data.

CHAPTER IV

SUMMARY

Based on the results of this study, NFT-NSS and FT-SS chamber emission rates were characterized by comparable systematic uncertainties in emission factor determination for both CH_4 and N_2O measurements. Source-specific methods require more labor compared to source-integrated methods for each measurement. The increase in labor is an issue for the source-specific methods if the intent is to collect a large number of samples to overcome the spatial heterogeneity of a large area sources. After averaging the emission factors calculated from each sample to account for spatial heterogeneity, the total systematic uncertainty increases to 75.9% and 84.96% for the NFT-NSS method and 87.6% and 53.0% for the FT-SS method when measuring CH_4 and N_2O, respectively. This increase was from the variation in concentration measured by each sample.

Source-integrated sampling techniques have an average systematic uncertainty of 15.2% when measuring CH_4 and N_2O because of the dominance of the air dispersion modeling required by each method to determine an emission rate. Specifically, the uncertainty in vertical dispersion as part of the air dispersion modeling dominates the uncertainty of the source-integrated methods. The uncertainty from the vertical dispersion coefficient could be reduced by utilizing the radial plume method with a monostatic FTIR system. OP-TDLAS is limited by the reduced number of compounds it is capable of detecting (including N_2O), but it is the least costly of the source-integrated methods and measures CH_4 more precisely than FTIR methods. OP-FTIR systems are capable of

measuring concentrations in real time, much like the OP-TDLAS, but are capable of measuring a vast array of compounds without the requirement of reference gases.

When source-specific and source-integrated methods are used simultaneously it is possible to more accurately determine emission factors than if either were used on their own. Source-specific methods are capable of individually characterizing the multiple sources of GHGs present in a large area source, while source-integrated methods account for the temporal and spatially heterogeneous aspect of large area sources.

An OP-FTIR system is a viable measurement device for characterizing GHG emissions from a large area source. The range of measured 1-hour average CH_4 concentrations were 1.62-6.87 ppm and 1.36-4.97 ppm for downwind and upwind measurements, respectively. Measured 1-hour average N_2O concentrations were 168-514 ppb and 203-530 ppb for downwind and upwind measurements, respectively. There was not a statistical difference between upwind and downwind measurements for N_2O. This was believed to be from the common use of nitrogen rich fertilizer in the surrounding area for grain production. The additional sources of N_2O drowned out any contributions to the measured concentration from the area source. Two OP-FTIR systems would be required to obtain more refined data for differentiation of the area source from surrounding sources two systems would be required. One OP-FTIR system would be placed downwind and the other upwind of the area source to produce a differential concentration.

With the dusty environment, it would have been preferred to house OP-FTIR system in a modified enclosed trailer with an opening that allowed for direct line of site

between the spectrometer and IR source. The manual tripod chosen for this study had too much play when locked to maintain alignment of the spectrometer and IR source during high wind events. In future studies, it is suggested to use a real-time positioning system with fine degree adjustments even though such a system may be costly. Stability of the spectrometer and IR source should be considered a priority and maintenance should be performed on a weekly or bi-weekly basis to obtain a consistent stream of usable data.

REFERENCES

ASTM Standards. 2007. E 1982: Standard Practice for Open-Path Fourier Transform Infrared (OP/FT-IR) Monitoring of Gases and Vapors in Air. West Conshohocken, PA: ASTM International.

Bjorneberg, D.L., A.B. Leytem, D.T. Westermann, P.R. Griffiths, L. Shao, and M.J. Pollard. 2009. Measurement of atmospheric ammonia, methane, and nitrous oxide at a concentrated dairy production facility in southern Idaho using open-path FTIR spectrometry. *Transactions of the ASABE*. 52(5): 1749-1756.

Boreal Laser. September 2010. Edmonton, Alberta. GasFinder 2.0. Available at: http://www.boreal-laser.com/products/gasfinder2. Accessed 27 January 2013.

Borhan, M.S., S. Capareda, S. Mukhtar, W.B. Faulkner, R. McGee, and C.B. Parnell. 2011. Determining seasonal greenhouse gas emissions from ground-level area sources in a dairy operation in central Texas. *Journal of the Air & Waste Management Association.* 61(7): 786-795.

Campbell Scientific. April 2011. Campbell Scientific, Inc.: North Logan, Utah.: CS100. Available at: http://campbellsci.com/cs100. Accessed 27 January 2013.

Campbell Scientific. June 2012. Campbell Scientific, Inc.: North Logan, Utah.: HMP60-L. Available at: http://campbellsci.com/hmp60-specifications. Accessed 27 January 2013.

Carslaw, D.C. and K. Ropkins. 2012. Openair – An R package for air quality data anylsis. *Environmental Modelling & Software.* 27-28: 52-61.

Cole-Parmer. 2011. Cole-Parmer. Vernon Hills, Il.: Mass Flow meter Model EW-32908-69. Available at: http://www.coleparmer.com/Product/Flowmeter_mass_differential_pressure _for_gases _0_05_to_5_L_min/EW-32908-69. Accessed 9 December 2011.

Cooper, C. David, and F.C. Alley. 2002. *Air Pollution Control.* 3rd ed. Long Grove, IL: Waveland Press, Inc.

Eggleston, S., L. Buendia, K. Miwa, T. Ngara, and K. Tanabe. 2006. Table 10.14. In *2006 IPCC Guidelines for National Greenhouse Gas Inventories.* Hayama, Japan: Institute for Global Environmental Strategies.

Eghball, B., and J. F. Power. 1994. Beef cattle feedlot manure management. *Journal of Soil and Water Conservation.* 49(2): 113-122.

Environmental Protection Agency (EPA. 1995. User's Guide for the Industrial Source Complex (ISC3) Dispersion Models. EPA-454/B-95-003b. Research Triangle Park, NC.: U.S. Environmental Protection Agency, Office of Air Quality Planning and Standards Emission Factors and Inventory Group.

Environmental Protection Agency (EPA). 2000. Meteorological Monitoring Guidelines for Regulatory Modeling Applications. EPA-454/R-99-005. Research Triangle Park, NC.: U.S. Environmental Protection Agency, Office of Air Quality Planning and Standards Emission Factors and Inventory Group.

Faulkner, W.B., J.M. Lange, J.J. Powell, B.W. Shaw, and C.B. Parnell. 2007. Sampler placement to determine emission factors from ground level area sources. *Atmospheric Environment* 41: 7672-7678.

Flesch, T.K., J.D. Wilson, L.A. Harper, R.W. Todd, N.A. Cole. 2007. Determining ammonia emissions from a cattle feedlot with an inverse dispersion technique. *Agricultural and Forest Meteorology* 144: 139-155.

FR 74 at 56373. Mandatory Greenhouse Gas Reporting. 74 Federal Register 209. 30 October 2009. 56373-56519.

FR 74 at 66496. Endangerment and Cause or Contribute Findings for Greenhouse Gases Under Section 202(a) of the Clean Air Act. 74 Federal Register 239. 15 December 2009. 66496-66546

Harper, L.A, T. Flesch, J. Poweel, W. Coblentz, W. Jokela, and N. Martin. 2009. Ammonia emissions from dairy production in Wisconsin. *Dairy Science* 92: 2327-2337.

Hashmonay, R.A., M.G. Yost, Y. Mamane, and Y. Benayahu. 1999. Emission rate apportionment from fugitive sources using open-path FTIR and mathematical inversion. *Atmospheric Environment* 33: 735-743.

Hashmonay, R.A. 2008. Theoretical evaluation of a method for locating gaseous emission hot spots. *Air & Waste Management Association* 58: 1100—1106.

Holman, Jack. 2011. *Experimental Methods for Engineers*. 8th ed. Columbus, OH: McGraw-Hill Education.

Intergovernmental Panel on Climate Change (IPCC). 2007. Climate change 2007: mitigation. Contribution of working group III to the fourth assessment report of the Intergovernmental Panel on Climate Change. Geneva, Switzerland: Intergovernmental Panel on Climate Change. Available at: http://www.ipcc.ch/ipccreports/ar4-wg3.htm. Accessed 15 Nov 2010.

Kawashima, H., M.J. Bazin, and J.M. Lynch. 1996. Global N2O balance and nitrogen fertilizer. *Ecological Modeling* 87: 51-57.

Kirchgessner, David A., S.D. Piccot, and A. Chadha. 1993. Estimation of methane emissions from a surface coal mine using open-path FTIR spectroscopy and modeling techniques. *Chemosphere* 26: 23-44.

Kyoung, S.R., P.G. Hunt, M.H. Johnson, A.A. Szogi, and M.B. Vanotti. June 2007. *Estimating ammonia and methane emission from CAFOs using an open-path optical remote sensing technology*. ASABE Paper No. 074004. Minneapolis, MN.: ASABE.

MIDAC. 2008. *Open Path Fourier Transform Infrared Spectrometry – User Manual*. Ver. 1. Westfield, Massachusetts: MIDAC Corporation.

Modrak, M., R.A. Hashmonay, R. Varma, and R. Kagann. 2005. Measurement of Fugitive Emissions at a Landfill Practicing Leachate Recirculation and Air Injection. EPA-600/R-05/088. Research Triangle Park, NC.: U.S. Environmental Protection Agency, Office of Air Quality Planning and Standards Emission Factors and Inventory Group.

Parkin, T.B., and R.T. Venterea. 2010. *USDA-ARS GRACEnet Project Protocols, Chapter 3. Chamber-Based Trace Gas Flux Measurements*. St. Paul, MN: USDA-ARS.

Reese, E., R.S. Martin, C. Going, E. Fowels, R. Sheffield, and M. Marti. June 2009. *Comparison of Ambient Ammonia Measurement Techniques from Dairy Area Sources*. ASABE Paper No. 095724. Reno, NV.: ASABE.

R Development Core Team. 2008. R: A language and environment for statistical computing. R Foundation for Statistical Computing, Vienna, Austria. ISBN 3-900051-07-0, URL http://www.R-project.org.

R M Young. 2011. R M Young Company: Traverse City, Michigan.: Ultrasonic Anemometer Model 81000. Available at: http://www.youngusa.com/products/11/3.html. Accessed 9 December 2011.

Rochette, P. 2011. Towards a standard non-steady-state chamber methodology for measuring soil N_2O emissions. *Animal Feed Science and Technology* 166-167: 141-146.

Russwurm, G.M., and J.W. Childers. 1996. FT-IR Open-Path Monitoring Guidance Document. EPA-600/R-96/040. Research Triangle Park, NC.: U.S. Environmental Protection Agency, National Exposure Research Laboratory Office of Research and Development.

Shores, R.C., D.B. Harris, E.L. Thompson, Jr., C.A. Vogel, D. Natschke, R.A. Hashmonay, K.R. Wagoner, and M. Modrak. 2005. Plane-integrated open-path fourier transform infrared spectrometry methodology for anaerobic swine lagoon emission measurements. *Applied Engineering in Agriculture* 21(3): 487-492.

Soleyn, K. 2009. Development of a Tunable Diode Laser Absorption Spectroscopy Moisture Analyzer for Natural Gas. Billerica, MA.: General Electric Company, GE Sensing & Inspection Technologies.

SRI. 2011. SRI Instruments. Menlo Park, Ca.: Gas Chromatograph Model 8610C. Available at: http://www.srigc.com/2005catalog/cat38-39.htm. Accessed 9 December 2011.

Taylor, B.N., and C.E. Kuyatt. 1994. Guidelines for Evaluating and Expressing the Uncertainty of NIST Measurement Results. Gaithersburg, MD: National Institute of Standards and Technology.

Thoma, E.D., R.C. Shores, and D.B. Harris. 2005. *Measurement of Ammonia Emission from Mechanically Ventilated Poultry Houses using Multipath Tunable Diode Laser Spectroscopy.* Research Triangle Park, NC: U.S. EPA.

Todd, R.W., N.A. Cole, K.D. Casey, R. Hagevoort, and B.W. Auvermann. September 2010. *Methane Emissions From A New Mexico dairy Lagoon System.* ASABE Paper No. 711P0510cd. Dallas, TX.: ASABE.

Turner, D.B. 1970. *Workbook of atmospheric Dispersion Estimates.* Washington DC. US Environmental Protection Agency.

Wanjura, J.D., C.B. Parnell, B.W. Shaw, and R.E. Lacey. August 2004. *A Protocol for Determining a Fugitive Dust Emission Factor from a Ground Level Area Source.* ASAE Paper No. 044018. Ottawa, Ontario, Canada: ASAE

Weiske, A, A. Vabitsch, J.E. Olesen, K. Schelde, J. Michel, R. Friedrich, and M. Kaltschmitt. 2005. Mitigation of greenhouse gas emissions in European conventional and organic dairy farming. *Agriculture, Ecosystems and Environment* 112: 221-232.

APPENDIX A

OPERATION OF THE MIDAC BISTATIC OP-FTIR

Scope: Outlines instrument setup, mirror alignment and data logging using the MIDAC bistatic OP-FTIR. This MOP includes instrument QC Procedures.

Purpose: To ensure correct instrument setup, mirror alignment and data logging using the MIDAC bistatic OP-FTIR.

Before deployment, perform all steps of *Pre-Deployment and QC Checks for bistatic OP-FTIR.*

PROCEDURE

1.1 General

The MIDAC bistatic system consists of physically separated infrared glow bars (Source) and interferometer (OP-FTIR). The Source and OP-FTIR must be transported to desired locations for acquisition of field data. The Source to OP-FTIR separation distance is rated up to 1,500 m (although we were unable to get good signal at 1,200 m at the Research Farm). Any distance outside of this range will require instrument preamplifier and attenuation settings which are not described in this operation procedure. Note that prior to acquiring field data, QC checks must be performed as outlined in section 1.5 through 1.7.

1.2 Source and OP-FTIR Connections, Setup and Log Preparation

1. Assemble the OP-FTIR spectrometer on the tripod and stabilize unit by lowering leveling legs. The instruments should be positioned to allow the field of vision of the 10” scope to be unobstructed by the protection cage. The tripod legs should then be stabilized on the floor plates.
2. Connect all cables on both the Source and OP-FTIR as detailed in steps 3 through 7. The cables and ports are labeled on the instruments are summarized in the table below.

Label No.	Port ID	Port Location
1	Computer 1	OP-FTIR Fiber Optic 1 (computer connection)
2	Computer 2	OP-FTIR Fiber Optic 2 (computer connection)
1	OP-FTIR 1	OP-FTIR Fiber Optic 1 (OP-FTIR connection)
2	OP-FTIR 2	OP-FTIR Fiber Optic 2 (OP-FTIR connection)
3	OP-FTIR Power Supply	OP-FTIR back Panel
S1	Source 1 Power Supply	Power Strip 1
S2	Source 2 Power Supply	Power Strip 2
S3	Source 3 Power Supply	Power Strip 3
S4	Relay Board Power Adapter	Power Strip 4
C1	Antenna	Cellular Modem

3. Plug the Source Power Supplies into the power strip inside of the Source access panel (3). The power adapter for the relay board that acts as switches for the Source should also be plugged into this power strip. Plug the power strip into an extension cable that goes to a power outlet.

4. Connect the two orange fiber optic cables (labeled 1, and 2) to the back of the OP-FTIR computer and of the OP-FTIR instrument. Note that the ports on both the computer and OP-FTIR instrument are also labeled 1 and 2.

    a. Once the computer is on, check that these connections are correctly made by opening AutoQuant and setting the instrument into align mode. If there is a lot of noise or a hardware error is received, reverse the connections.

5. Make the OP-FTIR computer connections (keyboard, mouse, and monitor). These are not labeled.

6. Connect the power for the computer, monitor and cellular modem (Raven XE) to the Power backup to ensure data integrity. Also connect the Power backup to the computer using a USB cable for monitoring of the device and automated shut down. DO NOT PLUG ANYTHING ELSE INTO THE POWER BACKUP.

7. Connect the computer to the modem using a Cat 5e LAN cable. Connect the antenna cable (labeled C1) to the modem on the port labeled "Antenna".

8. Mount the antenna at the top of the cage pointing in the direction of the nearest Verizon cellular tower. This can be found at http://www.cellreception.com/towers/gg.

9. Connect power supply to pig-tail on back of the interferometer (both are labeled “3”).

10. Connect power supply to a 110V power source.

11. Prepare the bistatic OP-FTIR Log book by attaching QC/Data Acquisition worksheet contained in Section 1.10. Record general field location description in log.

12. Acquire separation distance and bearing data of the Source to OP-FTIR using survey tape. Record values on QC/Data worksheet contained in bistatic Log.
13. Acquire GPS Data for the Source and OP-FTIR locations. Record values on QC/Data worksheet contained in bistatic Log.

1.3 Bistatic OP-FTIR Instrument Startup

1. Power-on the OP-FTIR computer followed by the OP-FTIR instrument. Note that a standalone gas generator may be required to provide power for the Source. Ensure that a battery backup system is used to provide clean, uninterruptible power to the OP-FTIR computer.
2. Open “AutoQuant Pro” software. Ensure that instrument is not in A/D overflow. If it is, check fiber optic connections.
3. Allow the system to warm-up for at least 60 minutes before acquiring data. Source alignment procedure can begin immediately but final adjustments to alignment must be made no sooner than 60 minutes after startup.
4. Power on the Source by following the steps below. (Note that a standalone gas generator may be required to provide power the Source).
    1. Open the ProXR software located on the desktop of the OP-FTIR computer.
    2. Select the radial button labeled Xbee ProXR and click “OK”. If this does not work check the Com Port selected at the top.
    3. Click the “Refresh” button until a choice other than "Broadcast to all devices" appears. If there are already two choices then choose the bottom one and click "Select". There will be a pause and a box will appear either saying the connection succeeded or failed. If it failed continue to click “Refresh” until the device reappears and click "Select" again. The computer may need to be restarted if the problem persists. Once the connection succeeds click "OK" and another window will open.
    4. In this next screen move the slider at the top of the screen all the way to the left so all devices are selected. Then the Source will be able to be controlled by clicking the buttons under Relay 1, 2 and 3.

1.4 Aligning the Source

1. See section 1.3 for Source, Computer, OP-FTIR and AutoQuant Pro startup procedures.
2. Remove all attenuating screens from the OP-FTIR Instrument.

3. Click on parameters and click "Align mode" on the left side of the window. Change the resolution to 8. Press “OK” at the bottom of the window.
4. On the Instrument tab, select “Align” on the left side of the window.
5. At least two persons are required for optical alignment of the Source and OP-FTIR. The operator of the OP-FTIR will watch the computer screen and note the signal intensity value during alignment. The alignment person(s) at the position of the source will physically move the source until a strong signal is acquired. Communication between the OP-FTIR operator and Source alignment person will be accomplished through use of two-way radios.
    a. Ensure that the Source and OP-FTIR trailers are resting properly on secure footings (with no weight on tires) and that the OP-FTIR is properly attached to its tripod. For long term applications the Source and OP-FTIR trailers should be secured with RV anchors. Set all vertical adjustments (telescoping tripod legs and vertical screw) to ensure an unobstructed field of vision for the spectrometer telescope and ensure that the protective cover has been removed from the telescope. Firmly lock all vertical adjustments.
    b. The OP-FTIR operator will double check to ensure that the attenuating screen is removed from the system.
    c. The OP-FTIR operator will sight from the OP-FTIR instrument to the Source to ensure that the systems are pointing at each other using a rifle scope installed on the OP-FTIR Instrument.
    d. The Source alignment person will sight from the Source to the OP-FTIR to ensure that the systems are pointing at each other using a rifle scope installed on the Source.
    e. The OP-FTIR operator will watch the computer screen and note the signal intensity value during alignment. The alignment person at the position of the source will adjust the pointing of the Source until a strong signal is acquired. Note that since the attenuating screen is not present, an A/D overflow condition may be registered. The system is now in rough alignment.
    f. After rough alignment has been achieved, the OP-FTIR operator will reinsert the proper attenuating screen (if used) and note the signal intensity level. An acceptable signal level is indicated by a Peak-to-Peak intensity between 4,000 and 40,000 (acceptable P/P is a function of source-to-spectrometer distance). If the signal level is too low, proceed to (g). If the signal level is too high, double check for proper placement and selection of attenuating screen. If the attenuating screen is correct, check to ensure that instrument gain setting has not been altered.

g. If all of these check out, turn off source and check for unusually high blackbody signal (should be below 2,500). Consult trouble shooting section 1.9. As a last resort, increase screen density and note the changes in the log book.

h. With a P/P signal level below 6,000 units, the alignment of the Source and OP-FTIR needs to be fine-tuned. First the Source alignment person will adjust the vertical tilt of the Source to maximize the alignment signal. Next the horizontal pointing angle of the Source will be adjusted to maximize signal. This procedure is repeated until optimized. (Rough rule of thumb: 60,000 P/P at 100 m and halves with every doubling of path length).

i. The OP-FTIR operator will then maximize the intensity signal through similar adjustments vertical tilt and horizontal pointing angle until the signal intensity level is optimized.

j. Repeat (h) and then carefully lock down the Source to prevent movement.

k. Repeat (i) and then carefully lock down the OP-FTIR to prevent movement.

6. Record the aligned power level with source on the QC/Data worksheet contained in the bistatic OP-FTIR Log book.

7. The system is now ready to perform quality control checks (Section 1.5 and 1.6) followed by field data acquisition measurements (Section 1.7).

1.5 Bistatic Instrument In-field, One Time Quality Control Checks

Because of the nature of the bistatic system, all quality control check are performed at the measurement path length. The Source and OP-FITR optical alignment must be optimized and the system must be warmed-up for at least 60 minutes before performing these checks. Refer to MOP-6807 section1.6 for test descriptions. **QC checks described in section 1.5 must be performed on a daily basis for short-term deployments (less than a month) and weekly for long-term deployments (greater than a month).**

1.5.1 Bistatic OP-FTIR Single Beam Ratio Test (SBR)

1. On the Instrument tab, select “Parameters” and click on “Align” to change the resolution to 0.5 cm^{-1}. Click “OK”.

2. On the left side of the screen in *AutoQuant*, select “Align”.

3. Allow *AutoQuant* to run for 60 seconds.

4. Record signal intensity (located in the first row of the "Best" column at the bottom left of the window in AutoQuant) level on the **QC worksheet** in the bistatic Log under "Initial Signal Intensity". Also record the location, date and time.

5. Click on the "Stop" icon to halt Alignment Scanning.

6. On the Instrument tab, select "Parameters" and click on "Scanning" to change the following settings.

    a. Sample Scans = 256

    b. Sampling Interval = As fast as possible

    c. Resolution = 0.5 cm^{-1}

    d. Save regions of interest = 550 to 4500 cm^{-1}

    e. Apodization = Triangle

    f. Phase correction = Mertz

    g. Gain = *1

    h. Laser wavelength: 0.63299 nanometers

    i. Zero Filling = 1x

    j. Click "OK"

7. On the left side of the screen click "Single".

8. Change the "Default Base Collection Directory" by clicking the "Browse" button and entering the following format "C:\date\QC" (e.g. "C: \060210\QC") into the box labeled "Folder".

9. Click "Open".

10. Click "Yes".

11. Change the subdirectory to "SBR".

12. Click "OK".

13. Calculate Ratio of intensity at 4000 cm^{-1} / 2000 cm^{-1} by dividing the Y-axis value at 4000 cm^{-1} by the Y-axis value at 2000 cm^{-1}.

14. Record Single Beam Ratio in QC worksheet contained in the bistatic OP-FTIR Log book. The Single Beam Ratio value must exceed 0.20 to be acceptable. If acceptable, proceed to section 1.5.2.

15. If the single beam ratio is below 0.20, proceed to section 1.9 for troubleshooting.

    Note: increment file name numerically for each separate acquisition on the same day.

1.5.2 Bistatic OP-FTIR Noise Equivalent Absorbance Test (NEA)

This quality control check is similar to that found in the *Pre-Deployment and QC Checks for bistatic OP-FTIR* but it is performed at the measurement path length. The scanning parameters have been chosen to minimize noise associated with normal atmospheric gas variations. A second purpose of this test is to look for the presence of intermittent noise events.

1. On the Instrument tab, select "Parameters" and click on "Scanning" to change the following settings:

    a. Sample Scans = 8

    b. Sampling Interval = As fast as possible

    c. Resolution = 0.5 cm^{-1}

    d. Save regions of interest = 550 to 4500 cm^{-1}

    e. Apodization = Triangle

    f. Phase correction = Mertz

    g. Gain = *1

    h. Laser wavelength: 0.63299 nanometers

    i. Zero Filling = 1x

2. Click "Storage "on the left side of the window.

    a. Click on the "Collect this many samples" radial near the bottom of the window.

    b. Change the value in the box to 5.

c. Click “OK”.

3. On the left side of the screen click “Continuous”.

4. Change the “Default Base Collection Directory” by clicking the “Browse” button and entering the following format “C:\date\QC” (e.g. “C: /060210/QC”) into the box labeled “Folder”.

5. Click “Open”.

6. If a window pops up saying the file does not exist then click “Yes”.

7. Change the subdirectory to “NEA”.

8. Click “OK”.

9. The Average value must be below 0.0004 and the maximum value must be below 0.0008 (Note these are trial values 7/28/04). If values are acceptable, proceed to section 1.5.3.

10. If the RMS values exceed these limits proceed to section 1.9 for troubleshooting steps.

1.5.3 Bistatic OP-FTIR Saturation of Instrument (Detector Nonlinearity) (SAT)

This quality control check is similar to that found in the *Pre-Deployment and QC Checks for bistatic OP-FTIR* but it is performed at the measurement path length.

16. On the Instrument tab, select “Parameters” and click on “Scanning” to change the following settings:

    a. Sample Scans = 32

    b. Sampling Interval = As fast as possible

    c. Resolution = 0.5 cm^{-1}

    d. Save regions of interest = 550 to 4500 cm^{-1}

    e. Apodization = Triangle

    f. Phase correction = Mertz

    g. Gain = *1

h. Laser Wavelength = 0.63299 nanometers

i. Zero Filling = 1x

17. Click “Storage” on the side of the window.

    a. Click on the “Continuous” radial.

    b. Click “OK”.

18. Click “Single” on the left side of the window.

19. Change the “Default Base Collection Directory” by clicking the “Browse” button and entering the following format “C:\date\QC” (e.g. “C: /060210/QC”) into the box labeled “Folder”.

20. Click “Open”.

21. If a window pops up saying the file does not exist then click “Yes”.

22. Change the subdirectory to “SAT”.

23. Click “OK”.

24. Zoom-in on region between 400 and 700 cm^{-1} are conduct flatness evaluation as described in MOP 6807-1.1.3. Record results in QC worksheet log.

1.5.4 Bistatic OP-FTIR Signal Strength (SS)

This quality control check is designed to ensure the FTIR is producing adequate data through interpretation of signal strength at various wavelengths of a single beam spectrum.

1. On the Instrument tab, select “Parameters” and click on “Scanning” to change the following settings:

    a. Sample Scans = 64

    b. Sampling Interval = As fast as possible

    c. Resolution = 0.5 cm^{-1}

d. Save regions of interest = 550 to 4500 cm^{-1}

e. Apodization = Triangle

f. Phase correction = Mertz

g. Gain = *1

h. Laser Wavelength = 0.63299 nanometers

i. Zero Filling = 1x

j. Click “OK”.

2. Click “Single” on the left side of the window.

3. Change the “Default Base Collection Directory” by clicking the “Browse” button and entering the following format “C:\date\QC” (e.g. C: /060210/QC) into the box labeled “Folder”.

4. Click “Open”.

5. If a window pops up saying the file does not exist then click “Yes”.

6. Change the subdirectory to “SS”.

7. Click “OK”.

8. Inspect the Single beam spectra at 3,500 ± 100 wave numbers on the X-axis to ensure that the signal exceeds 2,000 energy units on the Y-axis at any point within the region. Inspect the Single beam spectra at 1,000 wave numbers on the X-axis to ensure that the signal exceeds 6,000 energy units on the Y-axis. If either of these parameters are not met then check alignment by following the instructions in section 1.4. To zoom in on a region of the Single beam spectra, click and drag in the graph window to select the wanted region. To zoom back out, single-click again in the graph window.

1.6 Bistatic Instrument In-Field Daily Quality Control Checks

1. Perform all steps of Section 1.5 on a daily basis for short-term deployments (less than a month) and weekly for long-term deployments (greater than a month).

2. Refer to MOP 6807 for information on special post processing of data for daily QC checks.

1.7 Bistatic Instrument Field Measurements

Acquisition of field data cannot occur until all QC checks have been successfully completed (sections 1.5 and 1.6). The instrument must be warmed up, well aligned and with software started as described in sections 1.3 and 1.4. Note that the Peak to Peak signal intensity as determined in alignment mode is an important indicator of instrument alignment and must be monitored as described below and recorded in the QC/Data Acquisition worksheets in the bistatic Log.

1.7.1 Bistatic Data Acquisition Sequence

1. On line 1 of the **Data Worksheet** in the bistatic Log record the start date of data acquisition and the location with GPS coordinates and path length.

2. On the Instrument tab, select "Align" on the left side of the window.

3. Allow *AutoQuant* to run for 60 seconds.

4. Record Source on Signal Intensity (SI) level Peak to Peak reading on line 2a of the Data worksheet.

5. Record the time when the Signal Intensity reading was taken on line 2b.

6. Click "Stop".

7. Power down the source by following the steps below:
    a. Open ProXR, which can be done by double clicking the icon labeled ProXR on the computer desktop.
    b. Select the "Xbee ProXR" radial (If this is the second attempt to connect check the Com Port.
    c. Click "OK".

d. A new window will appear. Click “Refresh” until another option besides “Broadcast to all devices” appears. If there is already a second option it will not be required to click “Refresh”.

e. Select the second option and click “Select”.

f. After a short delay a window will appear indicating success or failure to connect. If it fails close ProXR, repeat steps a through e. If successful, click “OK”.

g. Two new windows will open. Move the top slider on the larger window all the way to the left so all channels are selected. The source power can then be controlled by clicking the buttons labeled “On” or “Off” next to Relay 1, 2 and 3.

8. Wait 30 seconds for readings to stabilize.
9. Go to AutoQuant and click on the “Instrument” tab.
10. Click “Align” on the left side of the window.
11. Record the Blackbody Signal Intensity level on line 3a.
12. Record the time when the signal intensity reading was taken on line 3b.
13. Click “Stop”.
14. On the Instrument tab, select “Parameters” and click on “Scanning” to change the following settings:

    a. Sample Scans = 64

    b. Sampling Interval = As fast as possible

    c. Resolution = 0.5 cm^{-1}

    d. Save regions of interest = 550 to 4500 cm^{-1}

    e. Apodization = Triangle

    f. Phase correction = Mertz

    g. Gain = *1

    h. Laser Wavelength = 0.63299 nanometers

    i. Zero Filling = 1x

15. Click “OK”.
16. On the Instrument tab, select “Single” on the left side of the window.

17. Change the Default Base Collection Directory by clicking the "Browse" button and entering the following format "C:\date\QC" (e.g. C: /060210/QC) into the "folder" box.
18. Click "Open".
19. If a question box appears click "Yes".
20. Change the subdirectory to "BB".
21. Click "OK".
22. Wait for scanning to complete then power up the Source using the instructions in part 1.7.1-6.
23. Go back to AutoQuant and click on the Instrument tab.
24. Select "Align" on the left side of the window.
25. Allow *AutoQuant* to run for 60 seconds.
26. Record the "Source on Signal Intensity" (The P/P signal) in line 5a.
27. Record the time when the signal intensity reading was taken on line 5b.
28. If signal intensity is in the acceptable range ((Rough rule of thumb: 60,000 P/P at 100 m and halves with every doubling of path length.) then proceed to 1.7.1-27, otherwise, optimize alignment as described in section 1.4.
29. Click "Stop".
30. On the Instrument tab, select "Parameters" and click on "Scanning" to change the following settings:
    a. Sample Scans = 64
    b. Sampling Interval = As fast as possible
    c. Resolution = 0.5 cm^{-1}
    d. Save regions of interest = 550 to 4500 cm^{-1}
    e. Apodization = Triangle
    f. Phase correction = Mertz
    g. Gain = *1
    h. Laser Wavelength = 0.63299 nanometers
    i. Zero Filling = 1x
31. Click "Storage" on the left side of the window.

a. Click on the “Continuous” radial.

b. Click “OK”.

32. On the Instrument tab, select “Continuous” on the left side of the window.
33. Change the Default Base Collection Directory by clicking the “Browse” button and entering the following format “C:\date\Data” (e.g. C: \060210\Data) into the “folder” box. Record this on line 6a on the **Data Worksheet**.
34. Click “Open”.
35. If a question box appears click “Yes”.
36. Leave the subdirectory as the default.
37. Click “OK”.

1.8 Bistatic Data Download

1. At the end of the run, download data to removable media.
2. Download mirror parameter file.
3. Erase files from computer only after successful transfer of data and mirror file to the EPA network.

1.9 Bistatic Instrument QC\Data Worksheet (to be secured in Biostatic Log)

QC Worksheet for bistatic FTIR (ver. 4/6/10)

Date:		
Location:		
QC Notes and Setup Description:		
Initial Signal Intensity:		Time:
SBR (1.6.1)	Ratio:	
NEA (1.6.2)	Avg.RMS: 985 = 2500 = 4500 =	Max RMA: 985 = 2500 = 4500 =
Sat (1.6.3)	Initial SI =	□ Pass or □ Fail

Data Worksheet for bistatic FTIR (ver. 4/06/10)

1. Data Sequence Notes:	
2a. Source on SI:	2b. Time:
3a. Blackbody SI:	3b. Time:
4a. Blackbody Filename:	
5a. Source on SI:	5b. Time:
6a. Data Sequence Filename:	

APPENDIX B

MAINTENANCE PROCEDURE FOR THE OP-FTIR: CLEANING OPTICS

The following procedure was used to clean the working optics of the open-path Fourier Transform Infrared Spectrometer system (OP-FTIR).

Tools Required

- 9/16” Socket
- 5/8” Socket
- Ratchet
- Set of Allen Wrenches (Metric and English)
- Distilled Water
- ½” wrench
- Extension cord

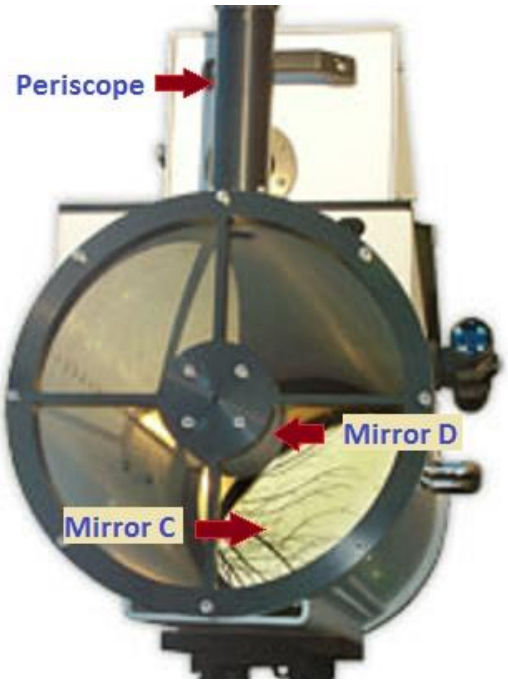

Figure 24. Shows the location of the periscope and the mirrors referenced in step 6-C and 6-D of the “Spectrometer Optics” Section.

Source Optics

1. On the trailer with the spectrometer (at the north-central point of the yard), open the orange JoBox by opening the locks under the duct tape.
2. Turn off the power to spectrometer by pressing the power switch on the black power supply in the JoBox.
3. Close the lid to the JoBox.
4. Undo the locks on the spectrometer cage.
5. Lean the door on the JoBox or take it off the trailer if extra clearance is needed to enter the cage.
6. Remove the air compressor and the air hose from the cage. Take these to the trailer with the source (at the northwest corner of the yard).
7. Connect the air compressor to the power pole using the extension cord (more than one may be required) or remove the back cover on the source and plug into the power strip there.
8. Make sure the air pressure is inhibited (30-50 psi) by the pressure regulator built in the air compressor for this operation. Also make sure the oil/water remover is connected to the air compressor.
9. Remove the bolts holding the screen on the front of the source.
10. Test the air nozzle to be sure that there is no water in the stream.
11. Spray the mirrors off using compressed air (no water in stream) initially to remove the majority of dust. Also spray out the interior of the source tube as much as possible.
12. Connect a bottle of distilled water to the venture setup and clean the mirrors thoroughly. Do not spray directly at the filaments in the middle (Be sure these are off before starting). Start at the top of the mirrors and work downwards.
13. Reinstall the screen and back plate of source (if removed).

Spectrometer Optics

1. At the spectrometer trailer, connect the air compressor to the power cord at the back of the trailer. Insert the tygon tubing connected to the air nozzle in a bottle of distilled water. (Keep this near the spectrometer cage as you will need it for step 6)
2. Switch off the compressor when not in use.
3. Enter the cage and move to the front of the spectrometer (the end farthest from the JoBox; shown in figure 24)
4. Carefully remove the periscope from the spectrometer (the brownish tube with a black cap on the top shown in figure 24). It is removed by unscrewing four (4) hex head screws with an Allen wrench. Once the screws are removed pull vertically. (Leave the periscope inside the cage) Once the periscope is off take the water bottle/spray nozzle setup and spray the compressed air until water from the water bottle flows through the air stream.
5. The pressure gauge on the air compressor should read between 35-50 psi when cleaning the mirrors. Adjust the pressure regulator to maintain less than 50 psi.
6. Four mirrors need to be cleaned on the spectrometer by spraying them with the compressed air/water stream. Multiple bottles of water may be required to clean the mirrors. **Do not touch the mirror surface with anything to refrain from scratching it!**
    a. First clean the mirror revealed from removing the periscope. This mirror is attached to a tube coming from the spectrometer underneath the periscope.
    b. Next clean the mirror inside the periscope and then turn the periscope with the black cap upward to allow the water to drain out.
    c. The next mirror to be cleaned is at the back of the large cylinder of the spectrometer. This is the largest mirror on the spectrometer (Mirror C in figure 24). Also clean the interior of the scope as much as possible.

    d. The last mirror to be cleaned is at the front of the large cylinder and is difficult to reach. There are two air nozzles available and should be alternated if necessary for the operators preference. (Mirror D in figure 24)
7. Once all four mirrors are clean, reinstall the periscope (if completely dry) using the four hex head screws. It will only fit one way.
8. Look through the hunting scope on the spectrometer and make note of where it is pointing with respect to the source (i.e. centered on the source, upper left corner of the source, etc.). Assuming the hunting scope is sited in properly; adjust the tripod to have the crosshairs of the scope in the middle of the source.
9. Take the tygon tubing out of the bottle of water and spray all the water out of the air line.
10. Place the air compressor and air hose in the cage.
11. Turn the power for the spectrometer back on by using the switch on the black power supply in the JoBox. Once this is done, log into the computer.
12. Turn on the source by the following steps on the computer:
    a. Open the ProXR software located on the desktop of the OP-FTIR computer.
    b. Select the radial button labeled Xbee ProXR and click “OK”. If this does not work check the Com Port selected at the top.
    c. Click the “Refresh” button until a choice other than "Broadcast to all devices" appears. If there are already two choices then choose the bottom one and click "Select". There will be a pause and a box will appear either saying the connection succeeded or failed. If it failed continue to click “Refresh” until the device reappears and click "Select" again. The computer may need to be restarted if the problem persists. Once the connection succeeds click "OK" and another window will open.
    d. In this next screen move the slider at the top of the screen all the way to the left so all devices are selected.

e. Click on the button labeled “OFF” under “Relay 1”, “Relay 2”, and “Relay 3”. At this time, the source should begin to glow.

13. Check alignment of the spectrometer by the following steps using the computer and tripod at which the spectrometer is attached:
    a. Open AutoQuant Pro on the located on the desktop of the OP-FTIR computer.
    b. Click “Align” on left side of the window in AutoQuant Pro.
    c. The spectrums flashing on the screen should look similar in shape to figure 25. Adjust the tripod to maximize the P/P number flashing underneath the spectrums. If the spectrums look similar to figure 26 then the spectrometer’s alignment is drastically off with the source or the source is not on (The source should be glowing orange).
    d. Once P/P is maximized, lock the tripod adjusters. Make sure the alignment is maintained after the tripod is locked.
14. Put the door back on the cage and replace the locks.
15. Perform start up procedures located in the “Operation of the Bistatic OP-FTIR.docx”.
16. Lock the JoBox and cover locks with duct tape.

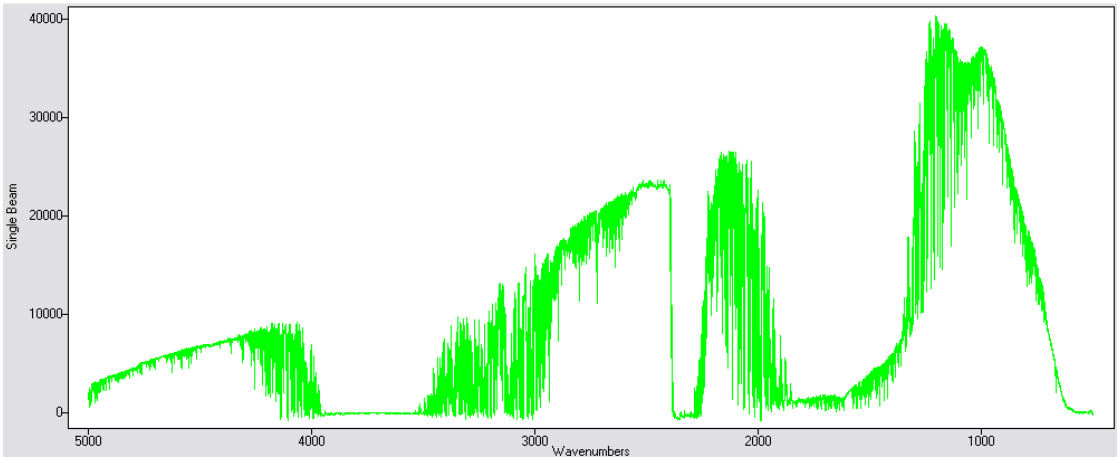

Figure 25. Spectrum representing a good alignment of spectrometer to source.

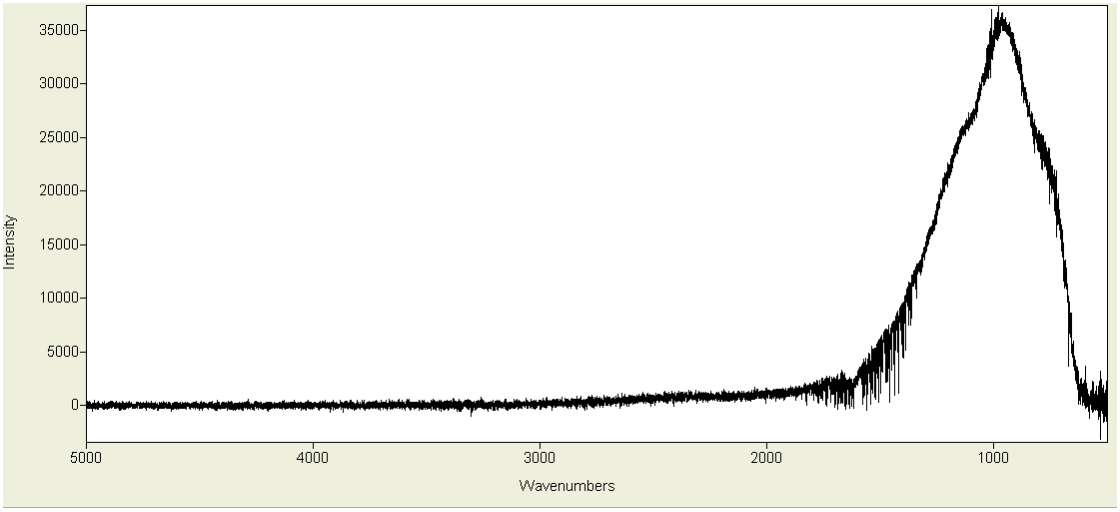

Figure 26. Example of Blackbody (represents poor alignment) spectrum.

APPENDIX C

AUTOQUANT PRO: METHOD DEVELOPMENT

Introduction

This document is designed to instruct new users to navigate the programs AutoQuant Pro (AQPro) and Essential FTIR (E-FTIR), in order to alter an existing AQPro method or create a new one from scratch. A method is required by AQPro to analyze the concentration of specific compounds assumed to be present in an absorbance spectrum. Once a method containing all compounds of interest is created, this method can be altered for different open-path Fourier Transform Infrared Spectroscopy (OP-FTIR) systems or if maintenance causes a variation in the x-shift of the original OP-FTIR system's output spectra. In the following portions of this document most situations which will require method refinement will be discussed and the process in which to carry out these refinements will be demonstrated. This document assumes reference spectra and field measurement spectra are readily available. Field measurements are assumed to be in the form of raw interferograms (IFG) and reference spectra unaltered.

Procedure

Converting Interferogram to Single Beam Spectra

1. Initially, the field measurement spectra in question need to be converted into Absorbance (ABS) spectra. To do this perform the following actions:
    a. Open AutoQuant Pro (AQPro).
    b. Click "Batch" located either on the left side or along the top bar of the AQPro window.
        i. If "Batch" was clicked on the top bar, a drop down window will appear with two options ("Batch" and "Re-Batch"), click "Batch"
    c. A new window with three (3) tabs will appear ("Batch Setup", "Storage", and "Background"). A brief explanation of each tab is included in the following

sub sections. To continue without these explanations, move to part “d” of this section.

i. The “Batch Setup” tab allows the user to select which spectra to process and whether to correct the Pathlength, atmospheric Temperature, and/or atmospheric Pressure. When converting IFGs to single beams (SB), these parameters must be corrected. More about utilizing these parameter corrections will be discussed in the following portions of this document.

ii. The “Storage” tab allows the user to choose the location in which the processed spectra will be saved and in what form (i.e. SB or ABS spectra). There is also an option to “Process only, do not analyze” the spectra. This option will convert the spectra to which ever form is selected without analyzing them for concentrations.

iii. The “Background” tab allows the selection of a background spectrum. This is a clean SB spectrum with a known concentration of the compounds in question. This spectrum will be ratioed with the field measurement SB spectra to create the ABS spectra for analysis. Since a spectra like this is unlikely to come by, these are created synthetically and will be discussed in more detail later.

d. On the “Batch Setup” tab click the “Browse” button.

e. Navigate to the location of the field measurement IFG spectra to be analyzed.

i. The IFG spectra file names will be displayed in the box in the center of the window.

ii. If the spectra file names are not being displayed be sure “Sample Interferogram (*.ifg)” is selected for “Files of Type” in the drop down box in above the box in the center of the window.

iii. Highlight all spectra to be converted to SB spectra, for the method development process select only one (1) spectrum. If all the files in this folder are to be selected, click the “Select All” button near the

bottom right side of the window. If analyzing large amounts of data, select intervals of one (1) hour worth of data (i.e. 1:00 to 1:59).

iv. Click the "OK" button on the bottom right side of the window.

f. Each time spectra are converted from IFG to SB, a correction of Temperature, Pressure, and Pathlength must be performed to produce accurate results. This can be performed at any transition period (i.e. period of converting spectra), but it is good practice to perform this step during the conversion of IFG to SB spectra. To perform these corrections execute the following steps:

   i. Obtain hourly averaged meteorological data for the time at which the spectra were collected and convert the values to the correct units (Celsius for Temperature, and Atmospheres for Pressure).

   ii. Check the three (3) boxes labeled "Over-ride individual file values with this value". If these boxes are not checked, the corresponding values will not be corrected.

   iii. Input the values for the Temperature and Pressure in the boxes labeled "Temperature" and "Pressure", respectively, that correspond to the time the spectra were collected. Input the path length, the distance between the spectrometer and the source, in the box labeled "Pathlength".

g. Click on the "Storage" tab.

   i. Click the "Browse…" button, a new window will appear. Navigate to the folder to save the SB spectra. Click "Open" once inside the folder. A new folder can be created to place the files in by clicking the button on the top of the window that looks like a folder with sparkles on the top right corner.

   ii. Check the boxes labeled "Save Single Beams" and "Process only, do not analyze". Uncheck all other boxes.

   iii. Click "OK" to begin the conversion.

iv. The window will close and another progress box will open. A single spectrum is being analyzed at this time, so the process will be very quick.

Creating a Synthetic Background

2. The SB spectrum created must now be converted to a synthetic background to create an absorbance spectrum. Open "My Computer" and navigate to the location where the SB spectra were saved.
    a. Open the SB spectrum to be created into a synthetic background in the program EssentialFTIR (E-FTIR).
        i. Backgrounds are created for every hour of data, so select the SB spectrum with the lowest minutes of an hour interval (i.e. 1:00). The background created will be utilized for the entire hour worth of data (i.e. 1:00 to 1:59) and then another background will be used.
    b. Click on the tab labeled "Manipulations" on the bottom left side of E-FTIR.
        i. Click "Smoothing in the window on the bottom left side of E-FTIR.
        ii. Set the following values in the corresponding boxes:
            1. "Smoothing Window" = 99
            2. "How to handle the end points" = "Fill with Zero"
            3. "Smoothing Method" = "Moving Average"
            4. Check the box labeled "Full Spectrum Smooth"
        iii. Click the button labeled "Apply to Current" three (3) times. If converting multiple SB spectra into synthetic backgrounds (i.e. for an entire day), click "Apply to All" three (3) times instead, as long as all spectra are open in E-FTIR.
        iv. Click "Zap" located on the bottom left side of E-FTIR.
        v. Set the following values in the corresponding boxes:
            1. "Fill With" = "Interpolated Line"
            2. "Add Noise" = 0.0

vi. Right click the in the spectrum window to add regions to zap. By left clicking and holding, a box can be created to zoom in on a specific location. Left clicking a single time with in the spectrum window will zoom back out. Add the regions displayed in figure 27. The regions will be roughly the same for every spectra, therefore, this can be done in a batch process to create a day's worth, 24, of synthetic backgrounds.

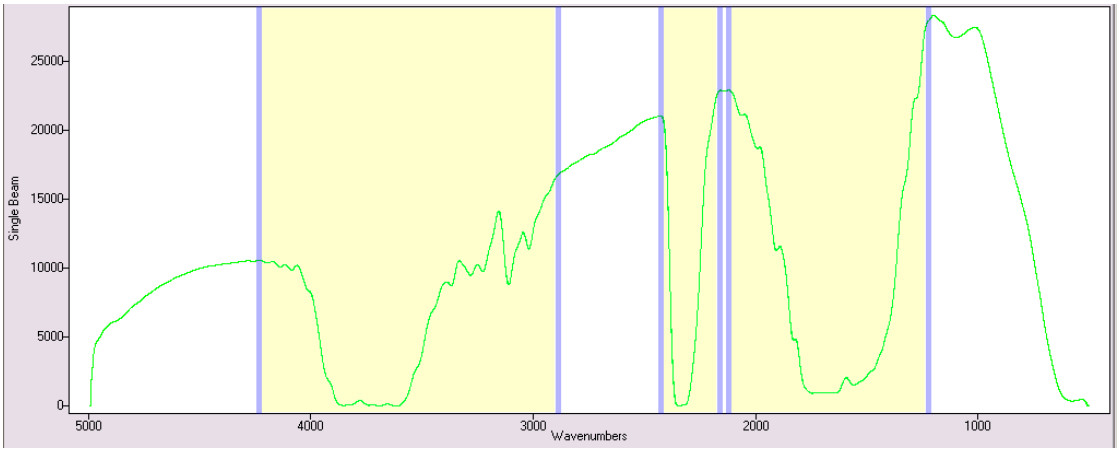

Figure 27. Demonstration of zap regions for the creation of synthetic backgrounds.

vii. If creating a single synthetic background, click "Apply to Current". If converting multiple SB to synthetic backgrounds, click "Apply to All".

viii. Save the spectra by clicking "Save As…". A window will appear where the location to save the spectrum can be chosen. Once chosen, click "OK".

1. If saving multiple spectra, click "Save". A dropdown menu will appear.
2. Click "Save to a Different Location"
3. Click "Save" again.

4. Click “Save All Files in Window” and a window will appear to select the location to save the spectra. Once chosen, click “OK”.

ix. Close E-FTIR

Converting Single Beam to Absorbance Spectra

1. Open AQPro.
2. Click “Batch” located either on the left side or along the top bar of the AQPro window.
    a. If “Batch” was clicked on the top bar, a drop down window will appear with two options (“Batch” and “Re-Batch”), click “Batch”
3. A new window with three (3) tabs will appear (“Batch Setup”, “Storage”, and “Background”).
4. On the “Batch Setup” tab click the “Browse” button.
    a. Navigate to the location saved SB spectra to be converted to Absorbance (ABS) spectra.
    b. The SB spectra file names will be displayed in the box in the center of the window.
        i. If the spectra file names are not being displayed be sure “Sample Single Beam (*.sb)” is selected for “Files of Type” in the drop down box in above the box in the center of the window.
        ii. Highlight all spectra to be converted into ABS spectra. If all the files in this folder are to be selected, click the “Select All” button near the bottom right side of the window. If analyzing large amounts of data, select intervals of one (1) hour worth of data (i.e. 1:00 to 1:59).
        iii. Click the “OK” button on the bottom right side of the window.
    c. Uncheck the three (3) boxes labeled “Over-ride individual file values with this value”, since the SB spectra have already been corrected.
    d. Click on the “Storage” tab.

i. Click the “Browse…” button, a new window will appear. Navigate to the folder to save the ABS spectra. Click “Open” once inside the folder. A new folder can be created to place the files in by clicking the button on the top of the window that looks like a folder with sparkles on the top right corner.
ii. Check the box labeled “Save Absorbance” and uncheck all other boxes.

e. Click on the “Background” tab.
i. Click the “Background…” button, a window will appear.
ii. Click the “Load from Disk…” button located on the new window, another window will open.
iii. Navigate to the location of the newly saved synthetic background spectra and change the “Files of type” to “Spectral Data Files (*.spc, *.abs)”.
iv. Select the spectrum that corresponds to the interval of data to be converted to ABS spectra (i.e. timestamp 0100 for the interval of 1:00 to 1:59).
v. Click “Open” once the spectrum has been selected and the window will close.
vi. Click “OK” to close the “Background Spectrum” window.
vii. Click “OK” to begin conversion process.
1. A progress window will appear and results will actively be displayed.
viii. Once finished, close AQPro.

Prepare Reference Spectra for Method Development

1. Open “My Computer” and navigate to the location of the saved ABS spectra.
2. Open a single ABS spectrum in E-FTIR.
3. Open “My Computer” and navigate to the location of the reference spectra.

4. The following steps must be performed for every reference spectrum for each compound to be included in the method. The images displayed in this section pertain to this process applied to a CH4 reference spectrum, but guidance will be provided for each compound currently observed.
    a. Open the reference spectrum to be x shifted in E-FTIR.
    b. Click on “Manipulations” on the left side of the E-FTIR window.
    c. Click on “X Shift” on the left side of the E-FTIR window.
    d. Zoom in to magnify the wave number range listed in table 12 below for the corresponding compound. (NH3 may not be present in the absorbance spectrum used for this operation, therefore, it may need to be x shifted at a later time when a spectrum is found where it is present).

Table 12. Zoom in range used to perform X Shift operations for reference spectra of various compounds.

Compound	Wave Number Range
Methane (CH_4)	2950 - 2946
Nitrous Oxide (N_2O)	2212 - 2210
Carbon Monoxide (CO)	2178 - 2175
Ammonia (NH_3)	1080 - 1064
Carbon Dioxide (CO_2)	2275 - 2272
Water Vapor (H_2O)	2948 - 2944

    e. Click on the name of the reference spectrum to alter in the top left portion of the E-FTIR window.
    f. For methane, the window should look similar to figure 28 below.

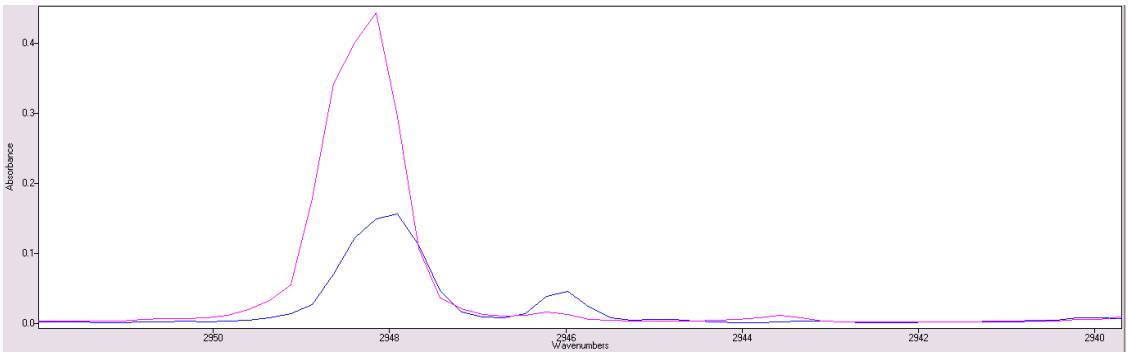

Figure 28. Example of zoomed in region of CH4 reference spectrum overlaid absorbance spectrum in E-FTIR.

g. The objective is to shift the reference spectrum, in the above figure this is the pink one, to where the peaks of reference and absorbance spectra match along the x axis. This is achieved by utilizing the labeled buttons in figure 29 below. The functions of these buttons are:
    i. Moves the selected spectrum to the right.
    ii. Moves the selected spectrum to the left.
    iii. Adjusts the sensitivity of movement utilizing “i” and “ii”.
    iv. Performs the designated shift value listed in the neighboring box.

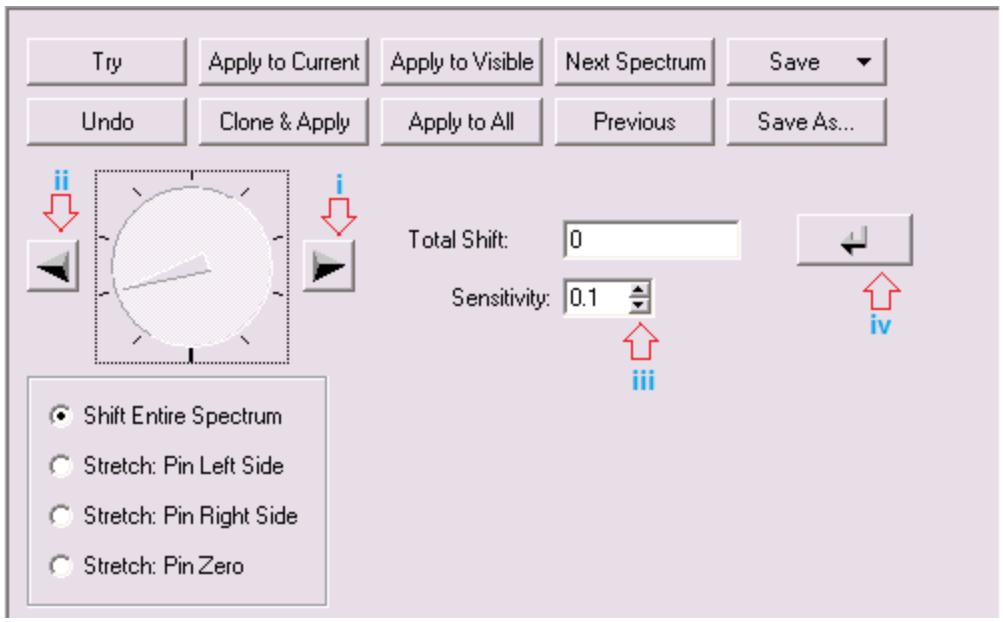

Figure 29. Buttons utilized to shift the spectrum.

h. Once a specific shift value is determined for a reference spectrum of a specific compound, the other reference spectra of the same compound likely will need to be shifted the same value. Therefore, the Total Shift button can be utilized for these other spectra as long as the same value is input in the neighboring box as was applied to the previous spectrum.

i. When adjustments are being performed a grey spectrum will appear in the window to show what the spectrum will look like before applying the changes, as seen in figure 30 below.

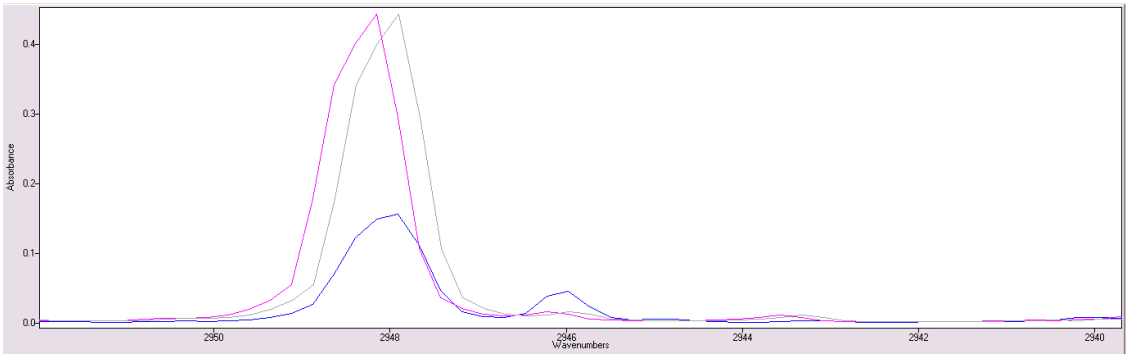

Figure 30. The grey spectrum is a preview the location in which the pink spectrum will be moved, based on current adjustments.

j. Once the peaks match for the reference and absorbance spectra match horizontally, click the "Apply to Current" button. This will move the reference spectrum to the position of the grey spectrum.
    i. If more adjustment is required, the previous steps can be repeated, or the "Undo" button can be utilized to undo the previous adjustment.
    ii. WARNING!! Make sure the reference spectrum is selected during these procedures and not the absorbance spectrum.
k. To save an individual spectrum, select the spectrum and click "Save As…".
l. Choose the location to save the selected spectrum in the window that appears and change the name to signify the changes. **Never save over the previous reference spectra!!!**
m. Repeat steps a – l for all the reference spectra to be included in the method.
n. Close E-FTIR when finished correcting all reference spectra.

Developing the Method

1. Open AQPro.
2. Click on "File" in the top left corner of the AQPro window. A drop down window will appear.
    a. Click "New Method…"

b. A new window, as shown in figure 31, will appear. Below is a description of each field that must be filled in before proceeding.

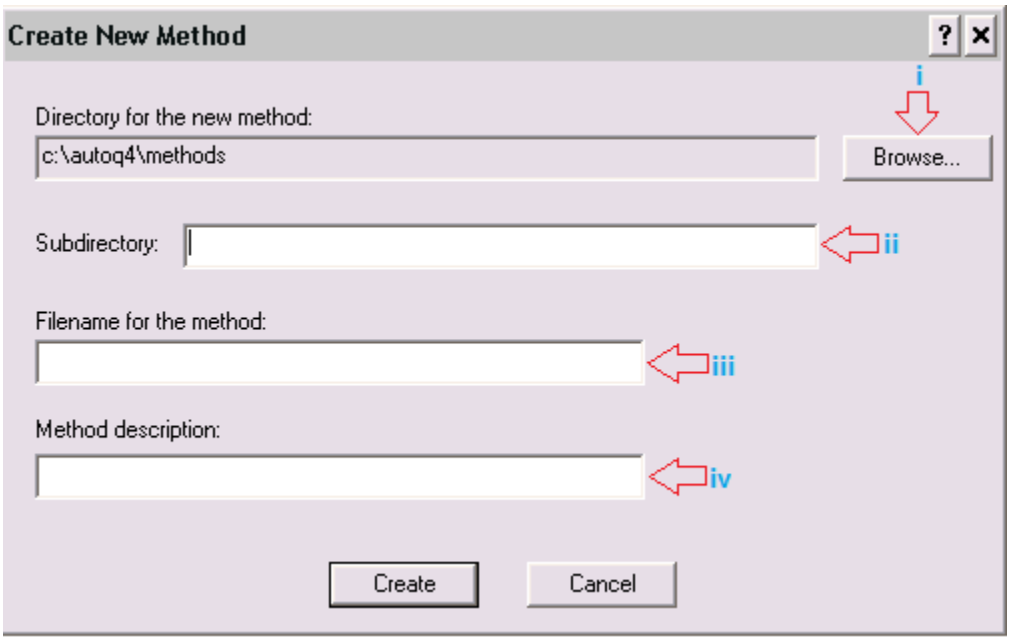

Figure 31. Window that appears during the process of creating a new method.

i. Click here first to choose the location to save the new method.
ii. Fill in this field with an appropriate name of the folder in which the method will be saved (i.e. FYC_South_Rev1, this example designates the method's use for the south FTIR system at Feed yard C and the number of revisions).
iii. Fill in this field with the same name as in the previous field.
iv. Fill in this field with any description of the method as seen necessary (i.e. the first revision of the method developed for the south FTIR system located at Feed yard C).

c. Once all fields have been completed, click "Create".

d. Click the tab labeled “Method” located below the image of the disk labeled “Save”.
e. To add a compound to the method, right click in the white area to the right of the label “Compounds”.
f. A drop down box will appear, Click “Add Compound…”.
g. A window will appear, as seen in figure 32 below. Fill in each field as described below.

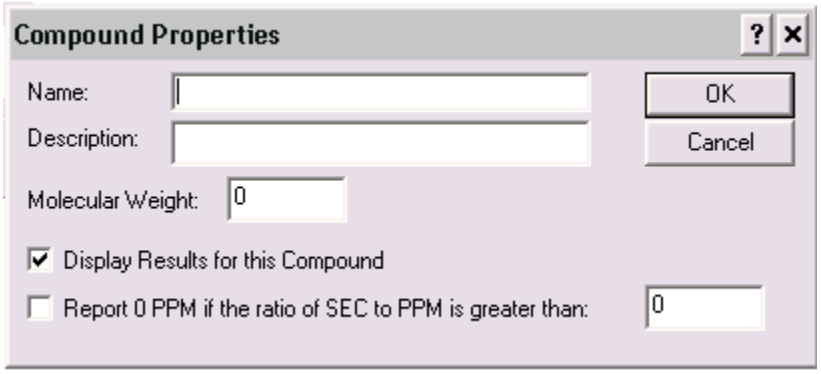

Figure 32. Window that appear when attempting to add a new compound to a method in AQPro.

i. Name: Enter the name of the compound to be added (i.e. CH4).
ii. Description: Enter a description of the compound to be added (i.e. Methane).
iii. Molecular Weight: Enter the Molecular Weight of the compound to be added (i.e. 16.04)
iv. For compounds that are included in the method strictly for their interference in the IR spectrum for compound of importance, uncheck the box labeled “Display Results for this Compound”. The reason for this is, the concentration of these compounds are not important and the addition of this data will create unnecessarily large excel files. For

all compounds of importance, leave the box labeled “Display Results for this Compound” checked.

v. Check box labeled “Report 0 PPM if the ratio of SEC to PPM is greater than:” and change the neighboring value to “1”. This will correct a concentration measured to zero if the standard error of concentration (SEC) is larger than the measurement. In other words, the error in measurement is larger than the measurement itself.

h. Once each field is filled out as described above, Click “OK”.

i. To add reference spectra associated with the compound added, right click in the white area to the right of the label “Spectra”.

j. A drop down box will appear, Click “Add Spectrum” and then Click “From Disk”.

k. Navigate to the location of the reference spectra for the associated compound and select one of the spectrums previously corrected through x shifting. Note: It is best to have at least three (3) reference spectra per compound, but this is not always possible. It is also best to choose reference spectra with concentrations close to the assumed concentration of the measurements. Each spectrum will need to be added separately.

l. Once a reference spectrum is selected, Click “Open”.

m. A new window will appear as shown in figure 33. Below is a description of each field.

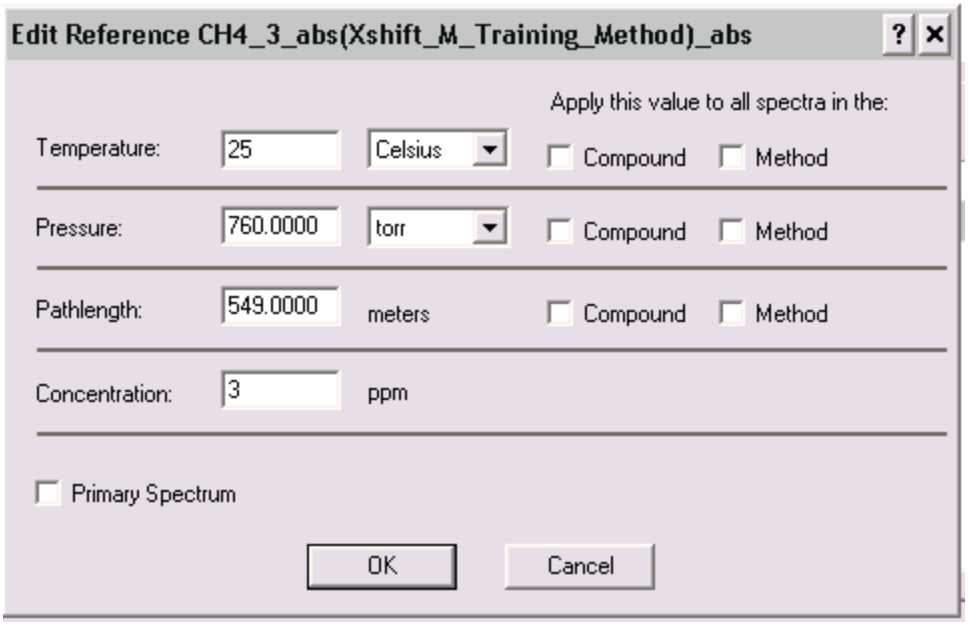

Figure 33. Window that appears when adding a reference spectrum to a method in AQPro.

i. Temperature: This will always be 25 C unless otherwise noted.
ii. Pressure: This will always be 760 torr unless otherwise noted in the name of the reference spectrum.
iii. Path length: This will be the path length at which the reference spectrum was created with and should be left as the default value.
iv. Concentration: The concentration will be listed in the name of the reference spectra (Except for water vapor). For example, in Figure 6 the name of the reference spectrum is "CH4_3_abs(Xshift_M_Training_Method)_abs". The concentration is listed after CH4, therefore, it is 3 ppm.
v. Primary Spectrum: This box must be checked for the reference spectrum that is closest to the expected concentration of field measurement.

n. Once all fields have been filled out adequately, click "OK".

o. Repeat steps i-o until all reference spectra desired have been added to the method as logical. No more than three (3) spectra should be added. At times there will only be one (1) spectrum available and this is fine.
p. To add regions in which AQPro will compare the reference spectra of a specific compound the analyzed spectra, right click in the white space to the right of the label “Regions”.
q. A drop down menu will appear, Click “Add Region”
r. A new window will appear.
    i. Select the compound in which editing is desired from the dropdown box labeled “Compound”.
    ii. Click the button labeled “New Region”
        1. Two (2) blanks will appear in the region table. Fill these blanks in with the appropriate values for each compound. These values can be found in table 13 below.

Table 13. Region values to input into new methods.

Compound	Region Start	Region End
Nitrous Oxide	2223	2174
Methane	2972	2862
Carbon Monoxide	2223	2174
Carbon Dioxide	2223	2174
Ammonia	980	957
Water Vapor	2972	2862
	980	957
	2223	2174

        2. Once a region has been added, click on the region in the region table and click “Apply to all Spectra in Compound”.
            a. Some compounds have multiple regions.
            b. CO2, CO, and Water Vapor are included in the method as interfering spectra with other compounds and have

similar regions to these spectra. It is important these compounds are included whether there is a desire to measure them or not.

3. Once all the regions for a compound have been added click "Done".

s. Repeat steps p-s until all compounds have the regions listed for them as noted in table 13.